

GROUND-STATE PROPERTIES AND MICROSCOPIC DESCRIPTION OF CLUSTERING IN ${}^6\text{He}$

Christian Forssén,
Fundamental Physics, Chalmers, Sweden

INT program 12-3, “*Light nuclei from first principles*”,
Seattle, Sep. 17 - Nov. 16, 2012



Main research funding by:



Outline

- ❖ Introduction - Ab initio towards the driplines
- ❖ Ground-state properties - Scales in NCSM
- ❖ A microscopic description of clustering
- ❖ Outlook - Stepping into the continuum

Ab Initio Towards The Driplines

From quarks to nuclei

Nuclear structure

Low-energy QCD

First step: Realistic interactions

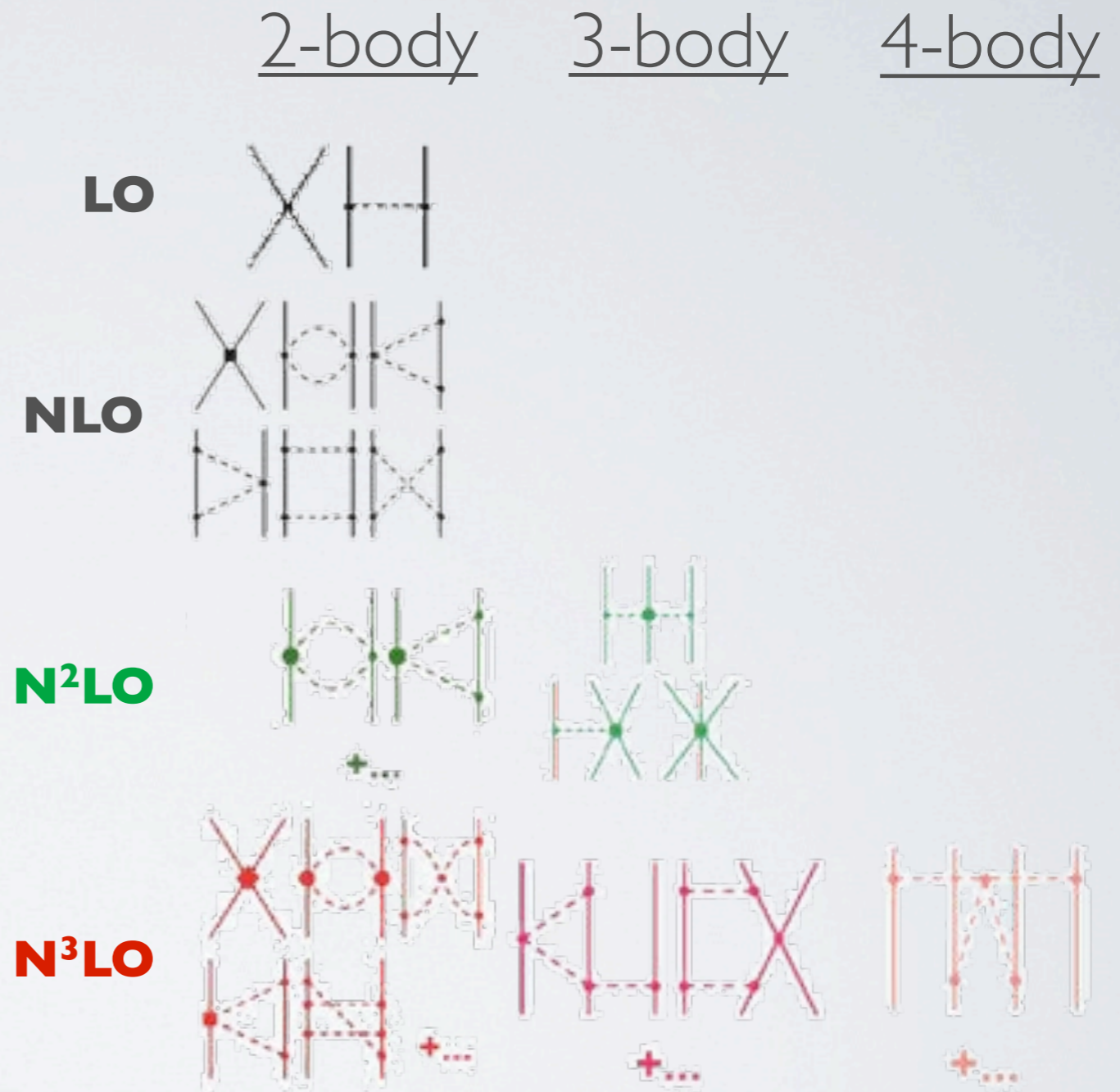
Nuclear structure

Realistic nuclear
interactions

Low-energy QCD

Chiral EFT-based nuclear Hamiltonians

- ❖ EFT for relevant degrees of freedom (π, N) based on symmetries of QCD
- ❖ Hierarchy of consistent NN, 3N, 4N, ... interactions
- ❖ See work by: Weinberg, van Kolck, Epelbaum, Meissner, Krebs, Entem, Machleidt, ...
- ❖ In the following we use:
 - ▶ NN: $N^3\text{LO}$ of Entem & Machleidt with $\Lambda = 500 \text{ MeV}$
 - ▶ 3NF: $N^2\text{LO}$



Chiral EFT

- E. Epelbaum, H. Hammer, U. Meissner Rev. Mod. Phys. **81** (2009) 1773
- R. Machleidt, D. Entem, Phys. Rep. **503** (2011) 1

Advanced many-body methods

Nuclear structure

Many-body methods



Realistic nuclear interactions

Low-energy QCD

A = 3,4: Several exact methods

- ▶ Faddeev-Yakubovsky, SVM, GFMC, HH variational, EIHH, NCSM
- ▶ Benchmark paper: Kamada et al, Phys. Rev. C64(2001)044001
- ▶ Very important observables for testing realistic nuclear Hamiltonians

A > 4: Very few (ab initio) methods available

Intermediate Step: Unitary Transformation

Nuclear structure

Many-body methods

Unitary transformations

Realistic nuclear interactions

Low-energy QCD

- ▶ adapt realistic potential to the available model space
- ▶ conserve experimentally constrained properties

Intermediate Step: Unitary Transformation

$$V(r) \propto g_1 \frac{e^{-\kappa_1 r}}{r} - g_2 \frac{e^{-\kappa_2 r}}{r}$$

$$\mathcal{F}_r(k - k')$$

↓

- ▶ Unitary transformation as a function of a flow parameter:

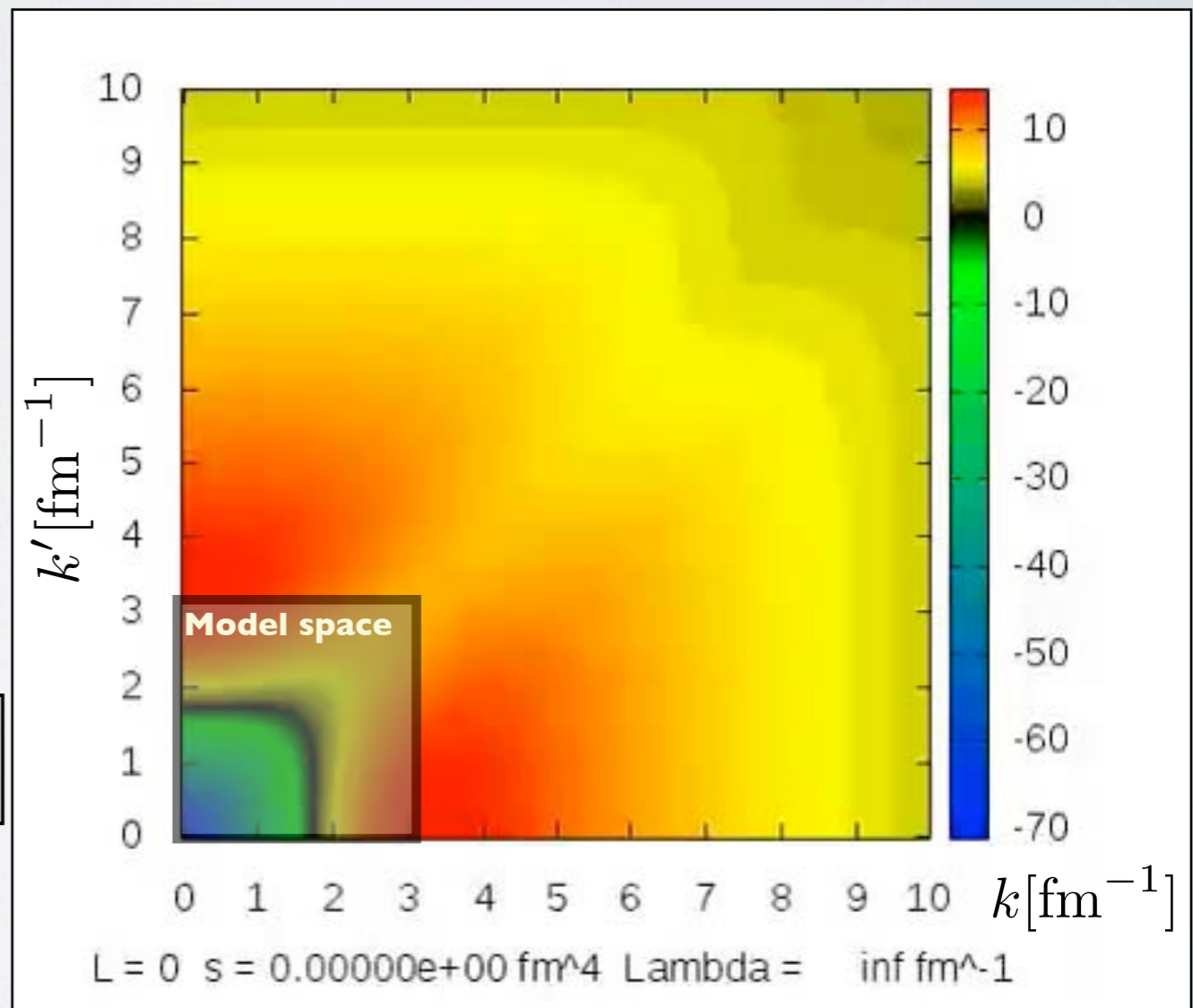
$$\tilde{H}_s = U_s^\dagger H U_s$$

- ▶ SRG evolution equation:

$$\frac{d}{ds} \tilde{H}_s = \left[\eta_s, \tilde{H}_s \right], \quad \eta_s \propto \left[T_{\text{int}}, \tilde{H}_s \right]$$

SRG

• S. Bogner, R. Furnstahl, A. Schwenk, Prog. Part. Nucl. Phys. **65** (2010) 94

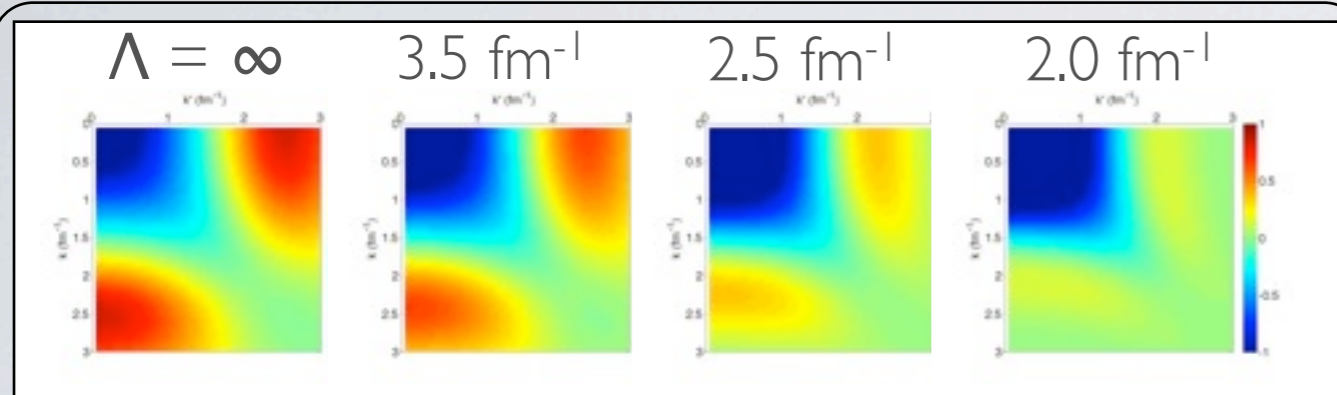


$\Lambda_{\text{HO}} = 20 \text{ MeV}; n = 17 \sim 3 \text{ fm}^{-1}$

C. Forssén, INT, Oct. 31, 2012

Effective-interaction approaches

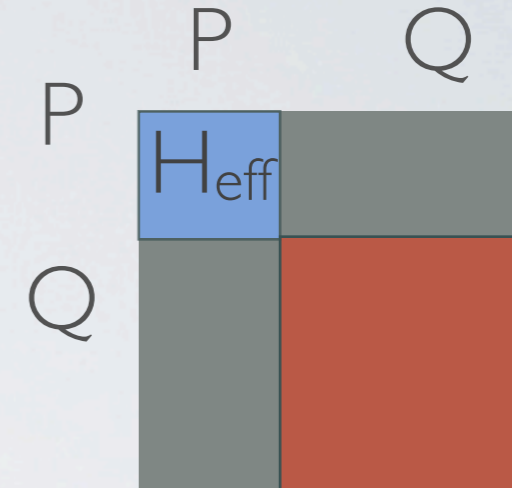
Bogner, Furnstahl, Schwenk, Prog. Part. Nucl. Phys. 65 (2010) 94



[SRG, V-UCOM, V-lowk.

[H_{eff} is independent of model space.

[Variational calculation
(but without A-body terms the converged result typically depends on the flow parameter)



[Lee-Suzuki-Okamoto

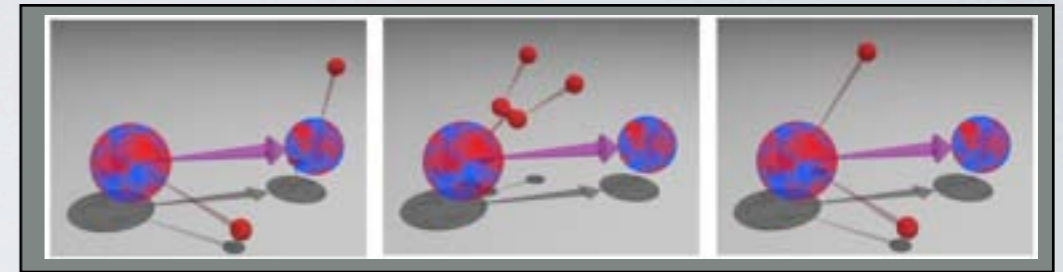
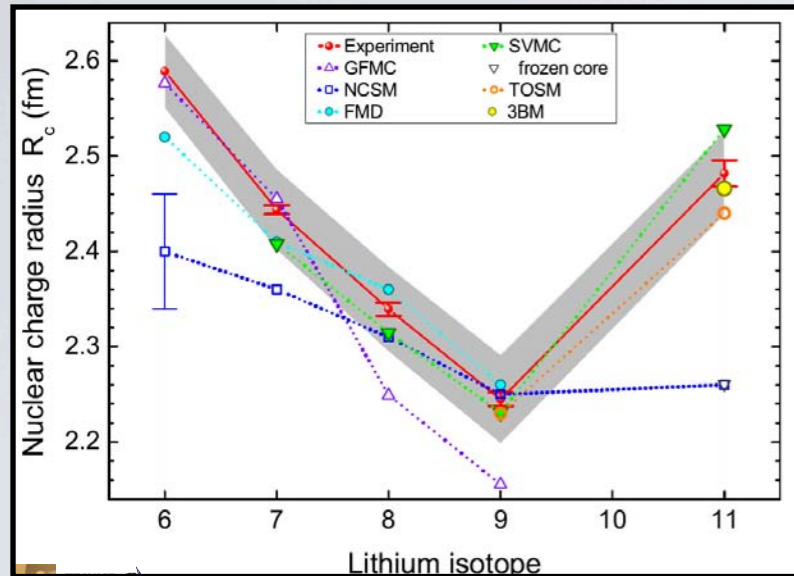
[H_{eff} is model-space dependent.

[Not variational
(but even with only 2-body terms it will converge to exact result)

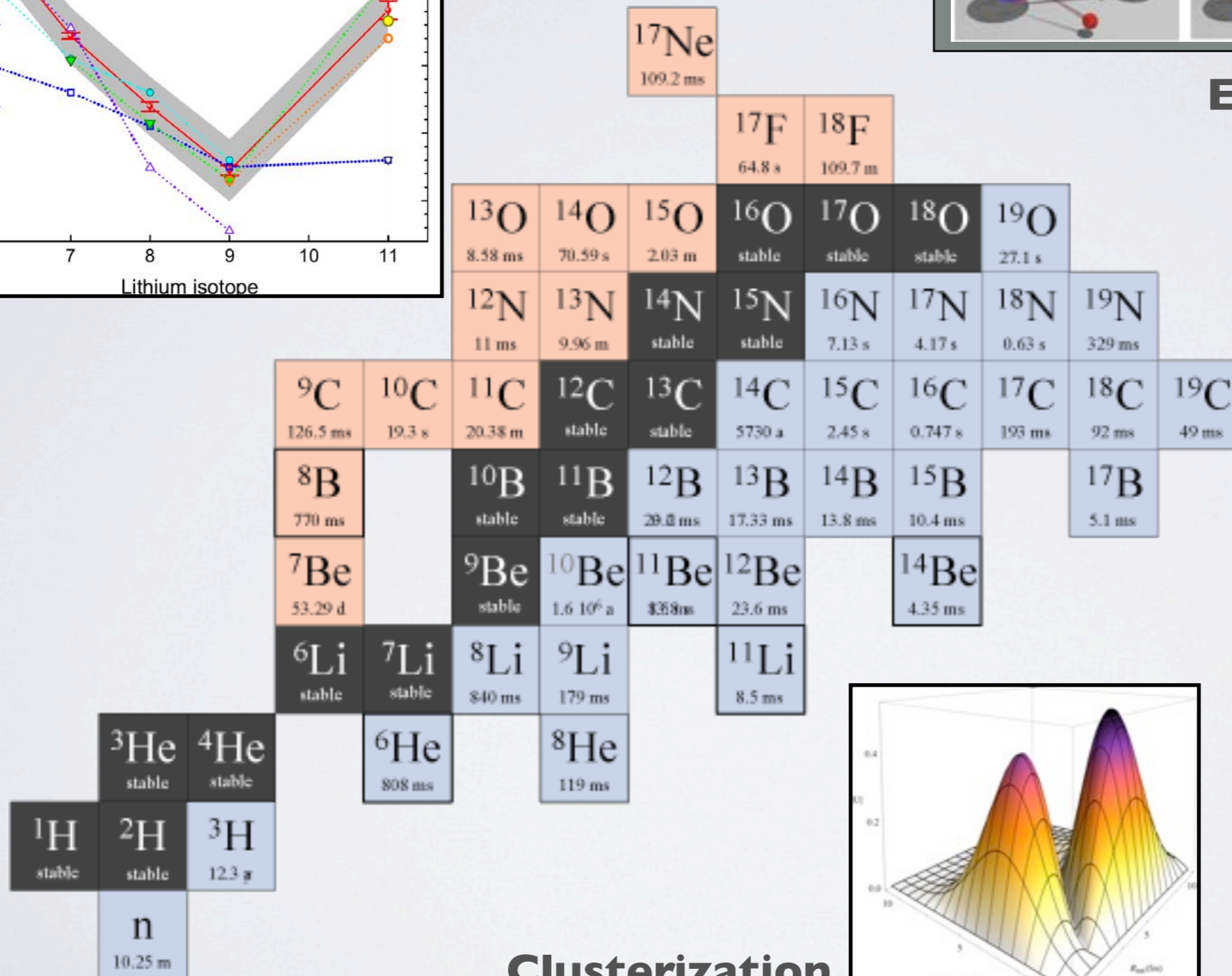
Many-body nuclear physics studied at low resolution scales comes at a price: the appearance of **many-body forces**.

Extremes of the (light) nuclear landscape

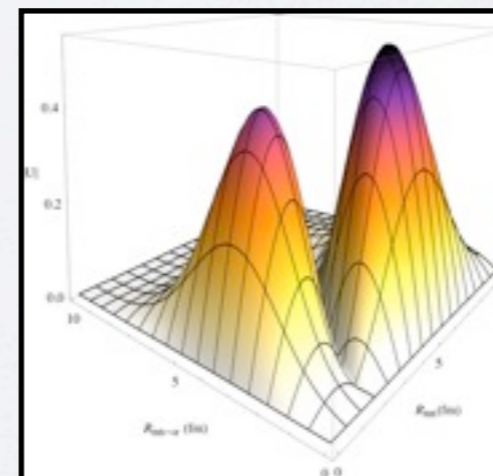
Observables: anomalous trends



Exotic decay modes



Clusterization



Halo states, Borromean systems

Ground-State Properties - scales in the NCSM

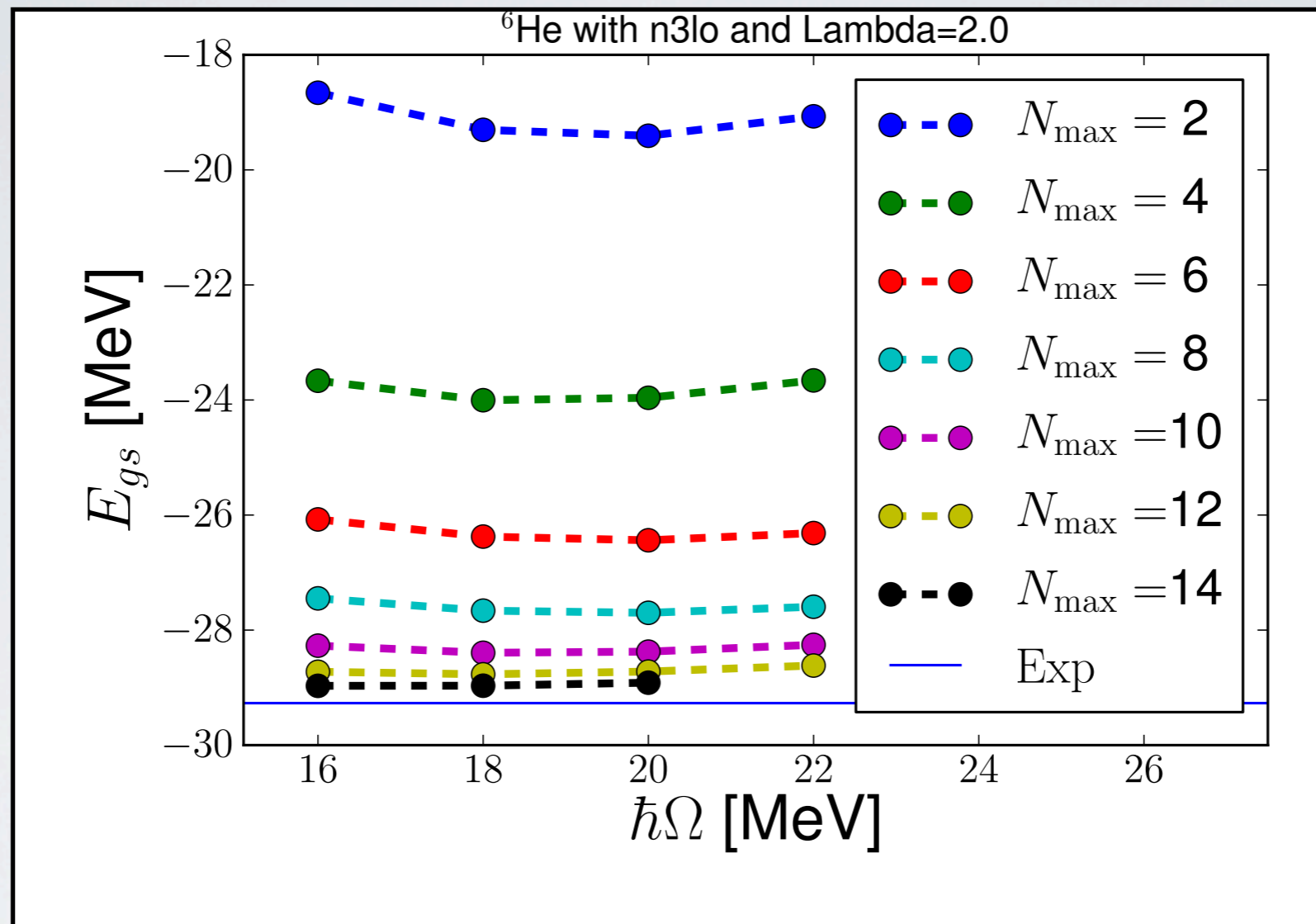
${}^6\text{He}$ Ground-State Properties

- ❖ Very accurate charge-radius measurements using laser spectroscopy.
- ❖ Very accurate mass measurement with a Penning trap mass spectrometer.
- ❖ Several ab initio calculations
- ❖ Most recently by S. Bacca et al
 - ▶ using EHH and V_{lowk} NN potential based on I-N³LO.
 - ▶ Study of V_{lowk} cutoff-dependence and observable correlations.

6-He references

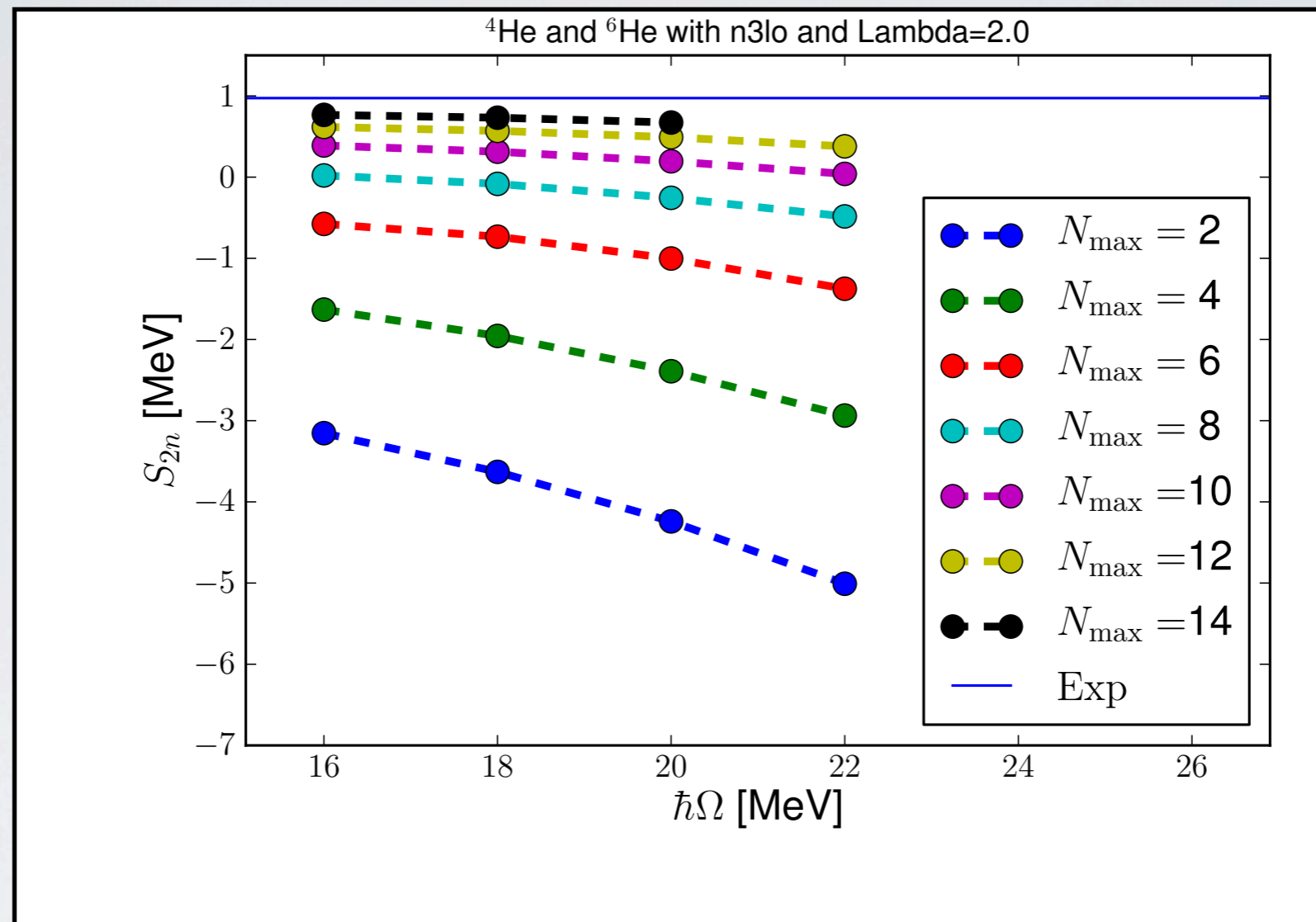
- P. Mueller et al., Phys. Rev. Lett. **99** (2007) 252501.
- M. Brodeur et al. Phys. Rev. Lett. **108** (2012) 052504
- S. Bacca. et al. Phys. Rev. C**86**, (2012) 034321

Ground-state energy of ${}^6\text{He}$



Typical variational pattern: large $\hbar\Omega$ cuts off wf and small $\hbar\Omega$ cuts off potential.
 \Rightarrow trade-off between IR and UV regulators

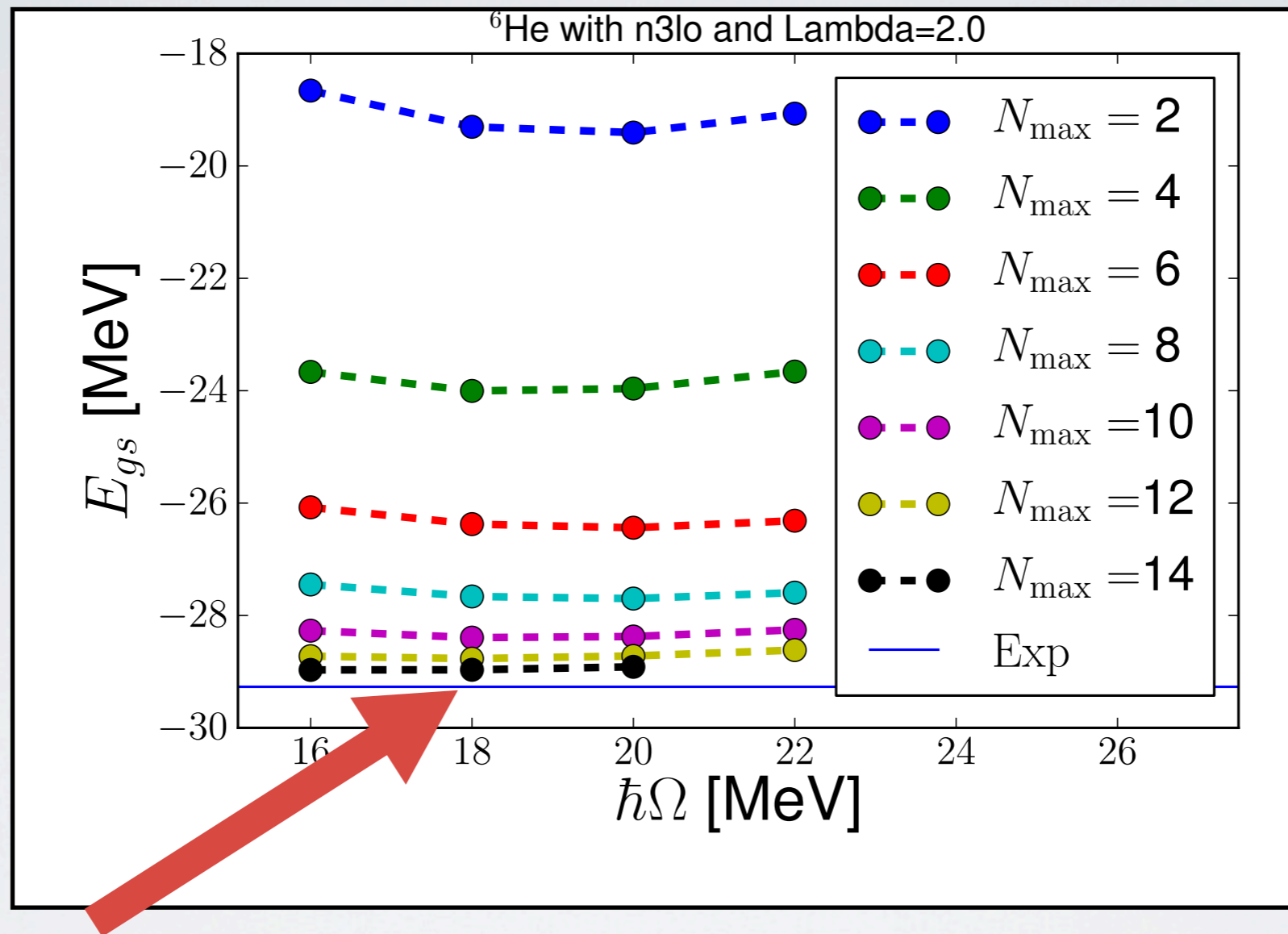
${}^6\text{He}$: Two-neutron separation energy



Note that no induced three-body terms were included
 \Rightarrow dependence on the SRG flow-parameter in these calculations.

Changes S_{2n} by approximately ± 200 keV in $[1.8, 2.2]$ fm^{-1} range

Ground-state energy of ${}^6\text{He}$

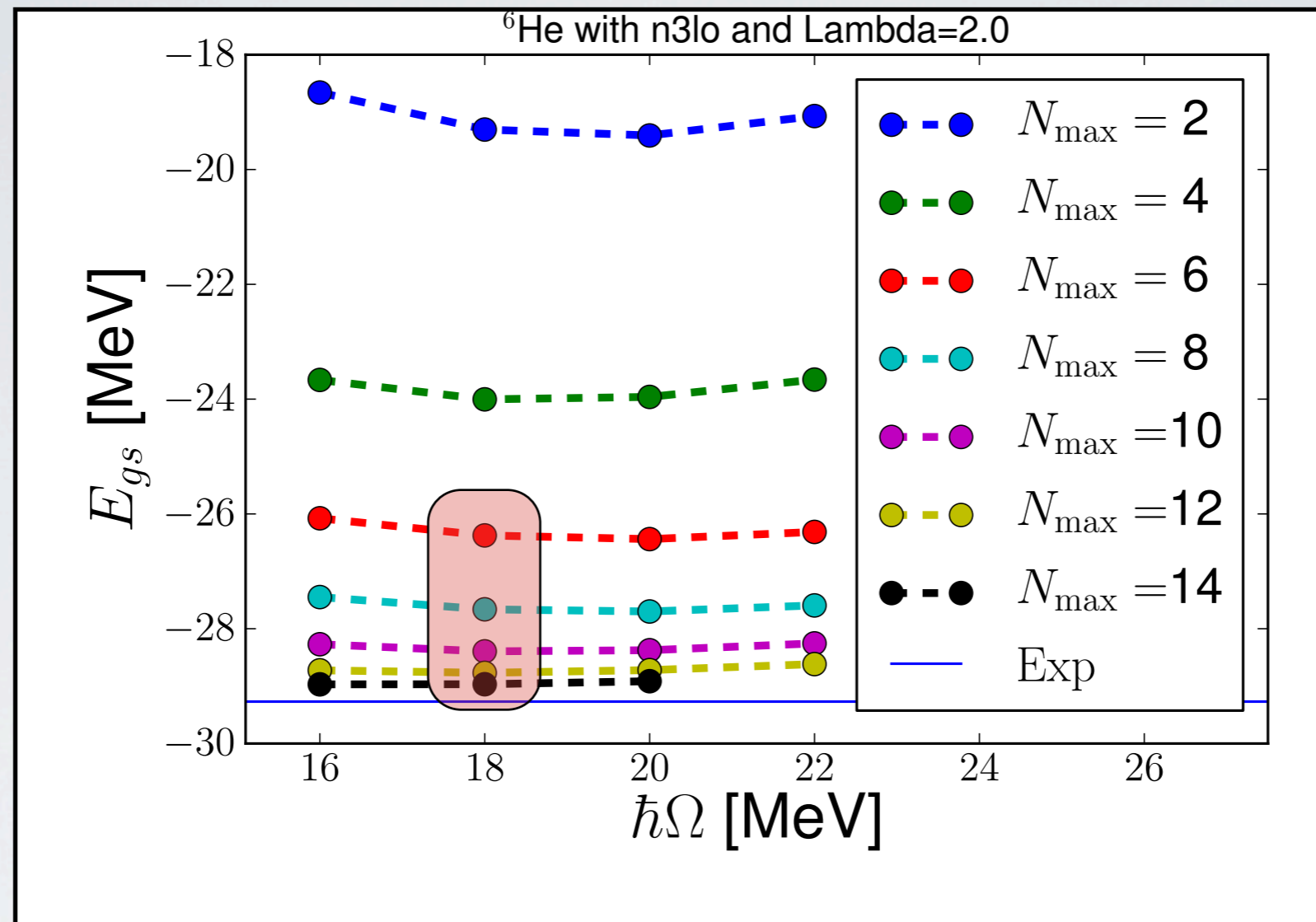


$E({}^6\text{He})$

-28.967 MeV

Single ($N_{\max}, \hbar\Omega$)

Ground-state energy of ${}^6\text{He}$

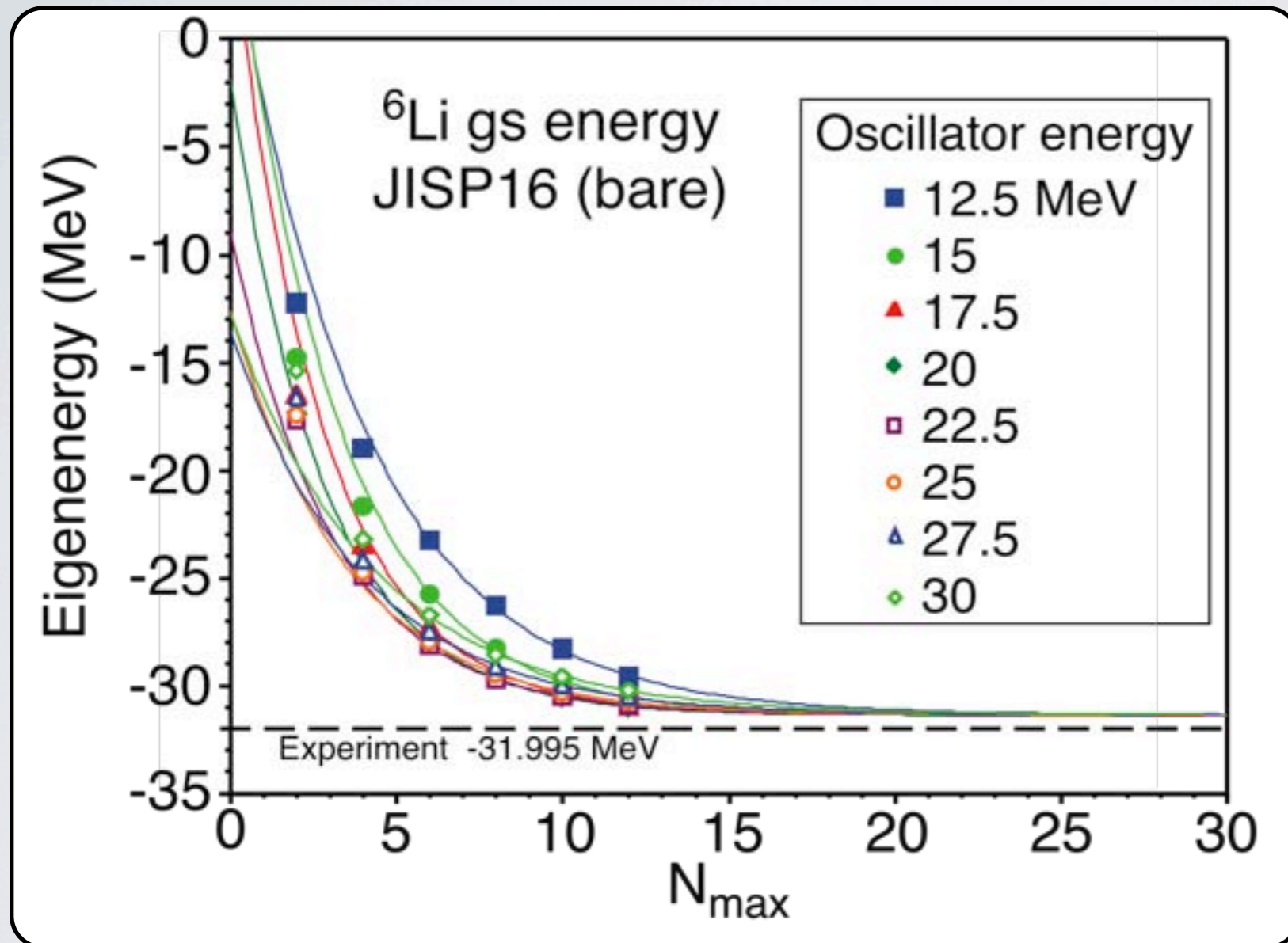


$E({}^6\text{He})$	-28.967 MeV	Single ($N_{\max}, \hbar\Omega$)
$E({}^6\text{He})$	-29.221 MeV	Exp. fit , Single $\hbar\Omega$

$$E(N_{\max}) = E_{\infty} + c_0 \exp(-c_1 N_{\max})$$

Converging sequences

Use results obtained at different HO frequencies to perform a **constrained fit**

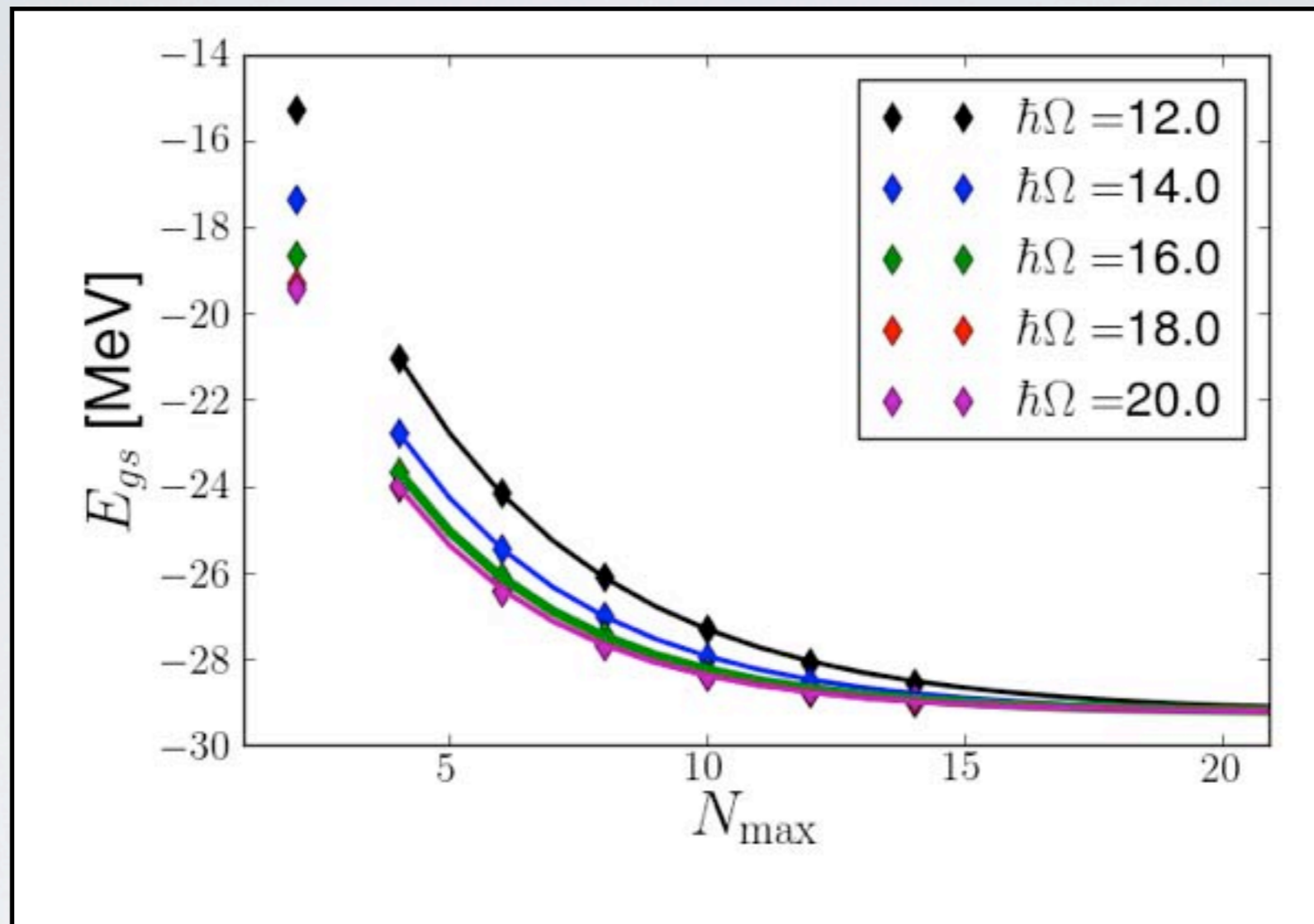


Powerful property

Any sequence that returns the initial Hamiltonian as the model space is increased will converge to the exact result.

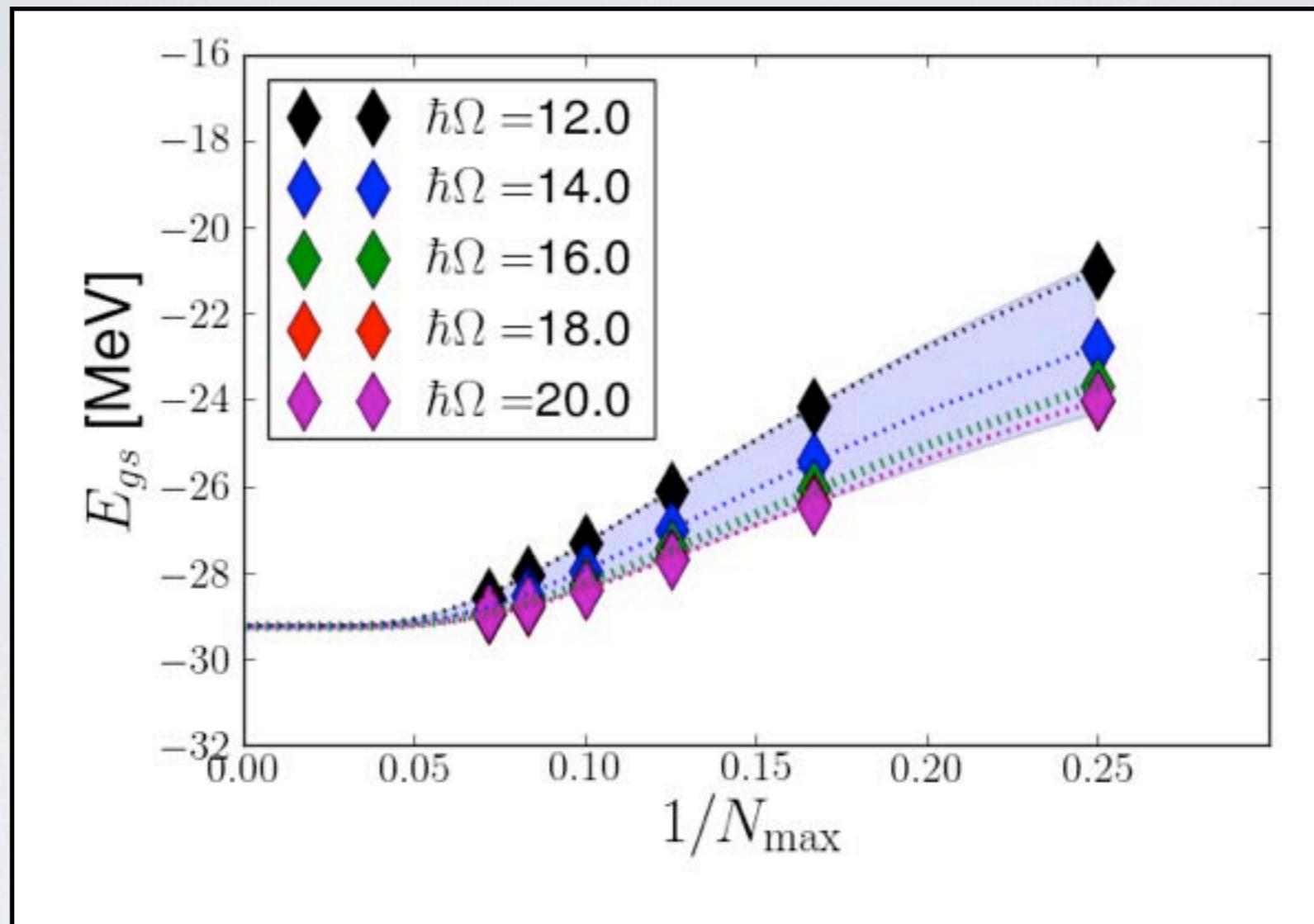
$$E(N_{\text{max}}, \hbar\Omega) = E_{\infty} + c_{0,\hbar\Omega} \exp(-c_{1,\hbar\Omega} N_{\text{max}})$$

Ground-state energy of ${}^6\text{He}$



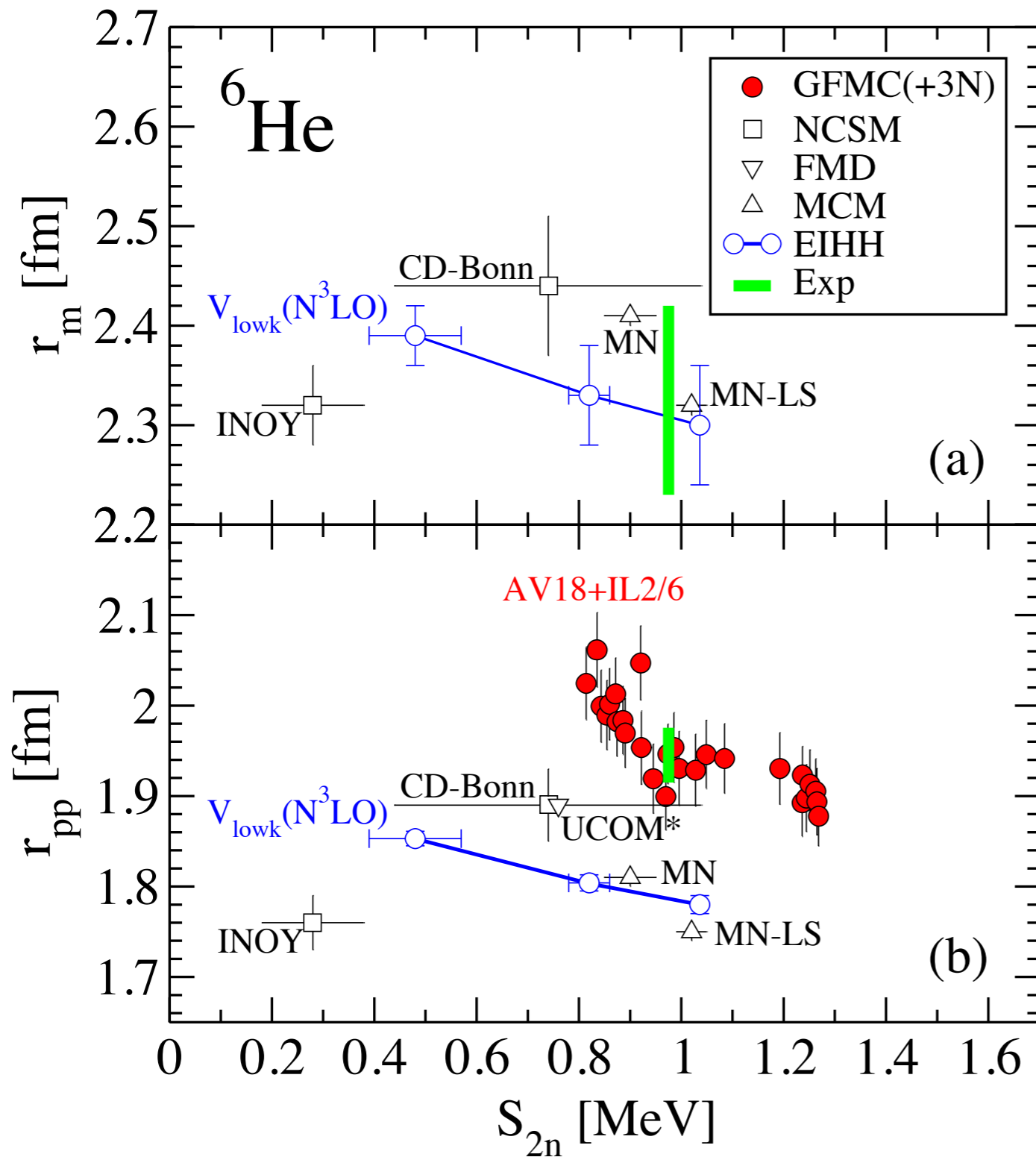
$E({}^6\text{He})$	-28.967 MeV	Single ($N_{max}, \hbar\Omega$)
$E({}^6\text{He})$	-29.221 MeV	Exp. fit , Single $\hbar\Omega$
$E({}^6\text{He})$	-29.240(93) MeV	Constrained fit

Ground-state energy of ${}^6\text{He}$



$E({}^6\text{He})$	-28.967 MeV	Single ($N_{\max}, \hbar\Omega$)
$E({}^6\text{He})$	-29.221 MeV	Exp. fit , Single $\hbar\Omega$
$E({}^6\text{He})$	-29.240(93) MeV	Constrained fit

${}^6\text{He}$ from EIHH



- Use hyperspherical coordinates, expand in HH and solve hyperradial equations

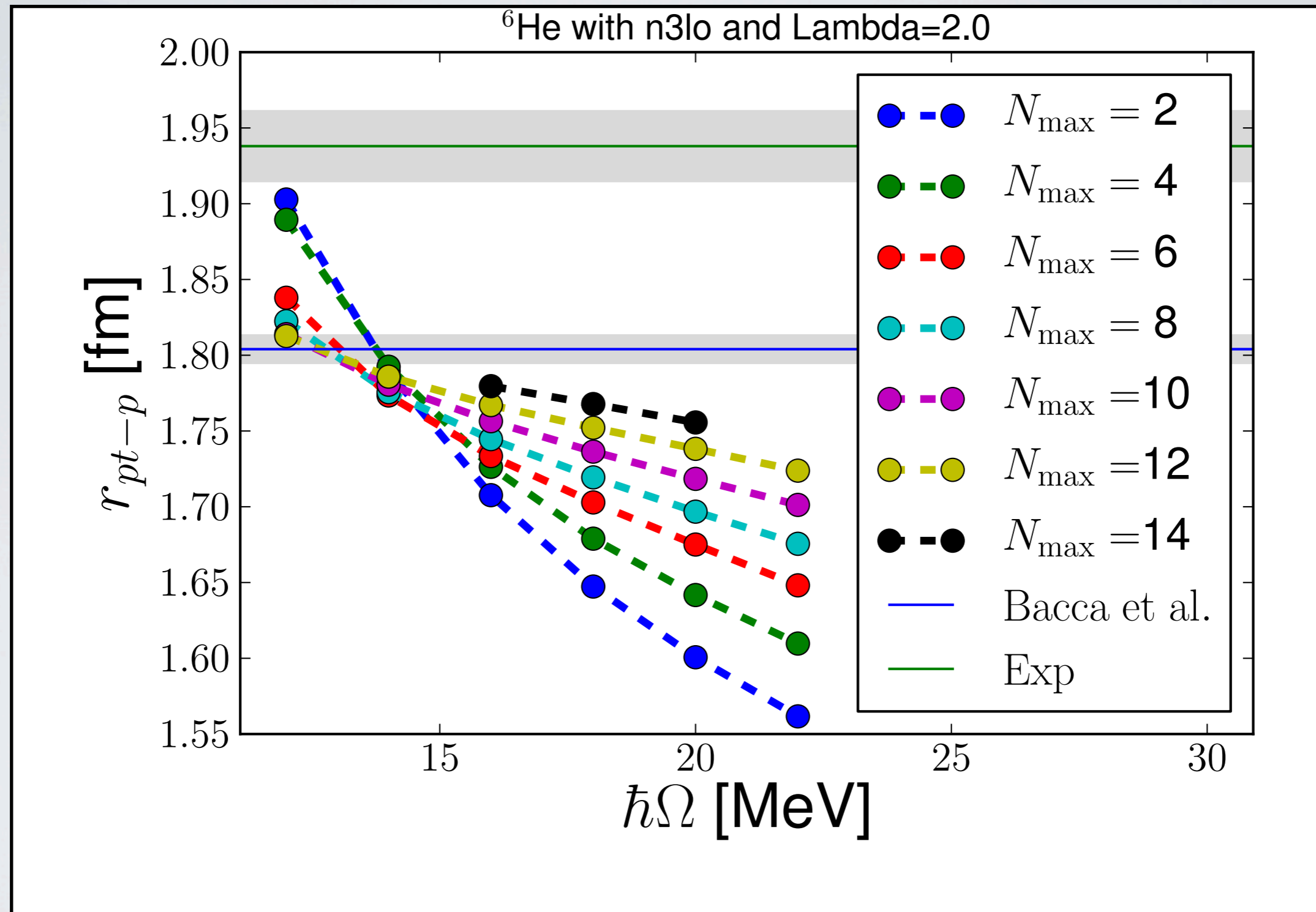
$$|\Psi\rangle = \sum_{[K]} \sum_{\nu}^{K_{\max} \nu_{\max}} c_{[K],\nu} \mathcal{Y}_{[K]}(\Omega) e^{-\rho/2b} L_{\nu}(\rho)$$

- $V_{\text{low-k}}$ from I-N3LO with various cutoffs Λ
- Lee-Suzuki effective interaction
- Study correlations of observables

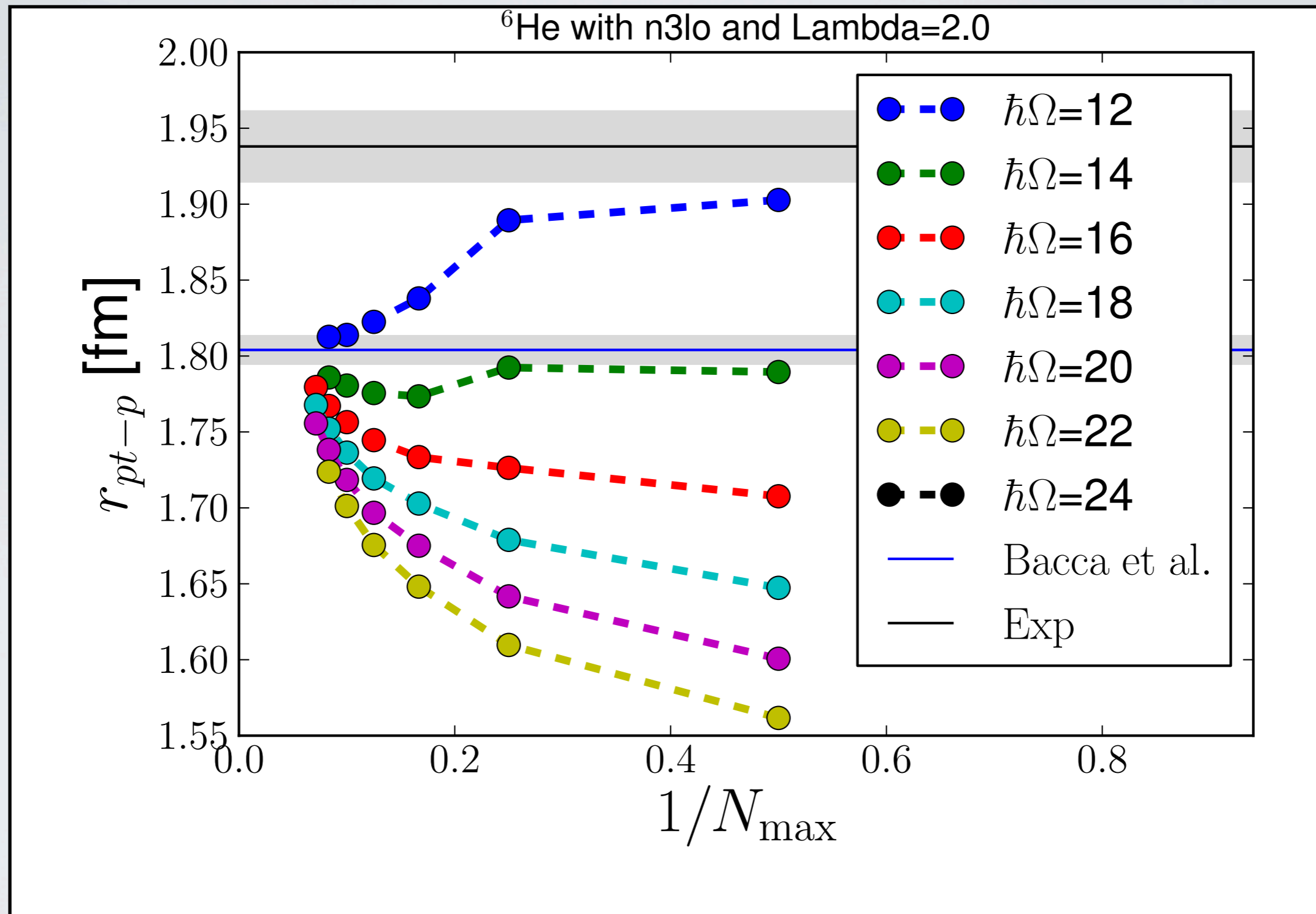
6-He measurement and EIHH calculations

- M. Brodeur et al. Phys. Rev. Lett. **108** (2012) 052504
- S. Bacca. et al. Phys. Rev. C **86**, (2012) 034321

${}^6\text{He}$: Point-Proton Radius

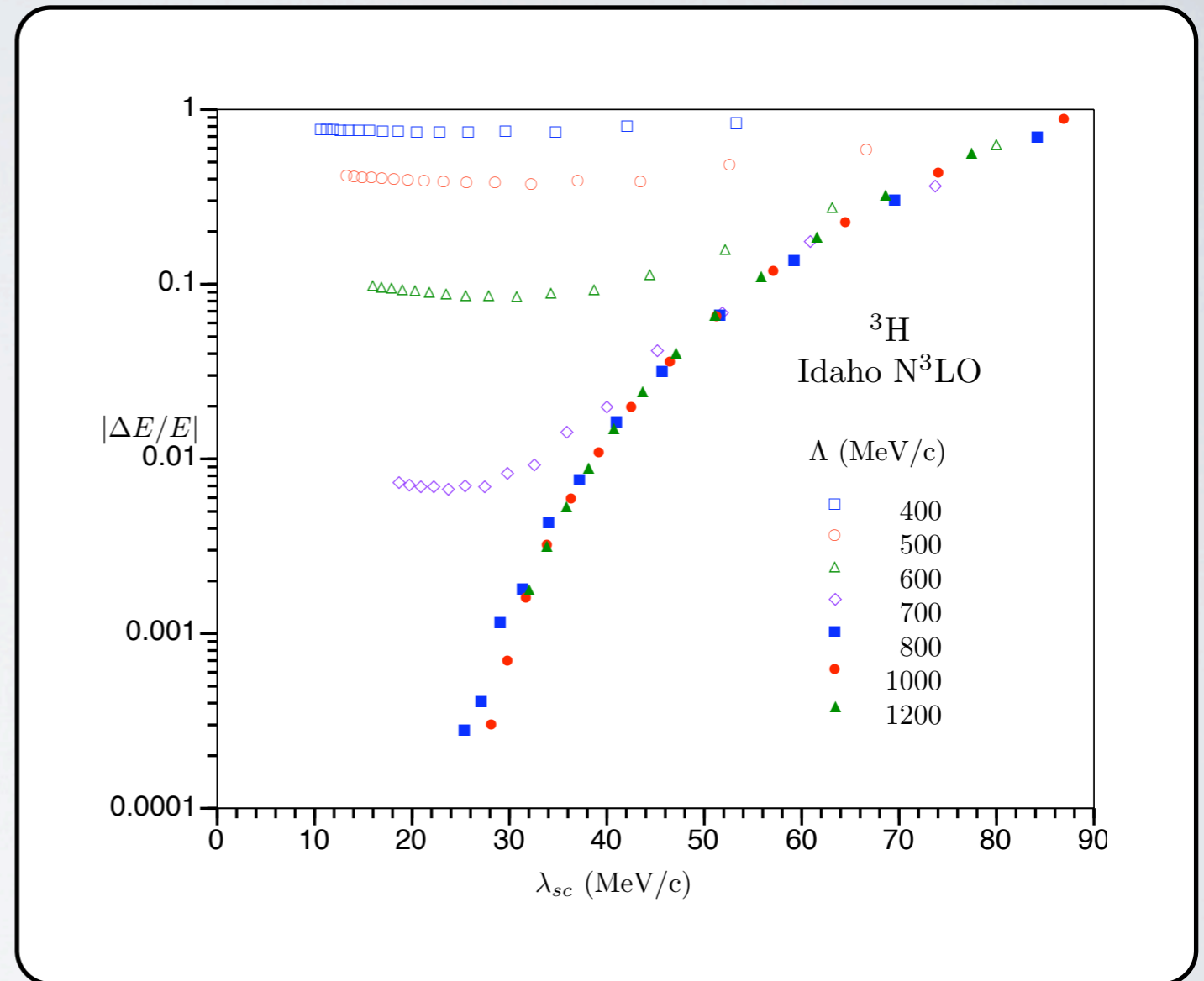


${}^6\text{He}$: Point-Proton Radius



Switching to IR and UV cutoffs as variables

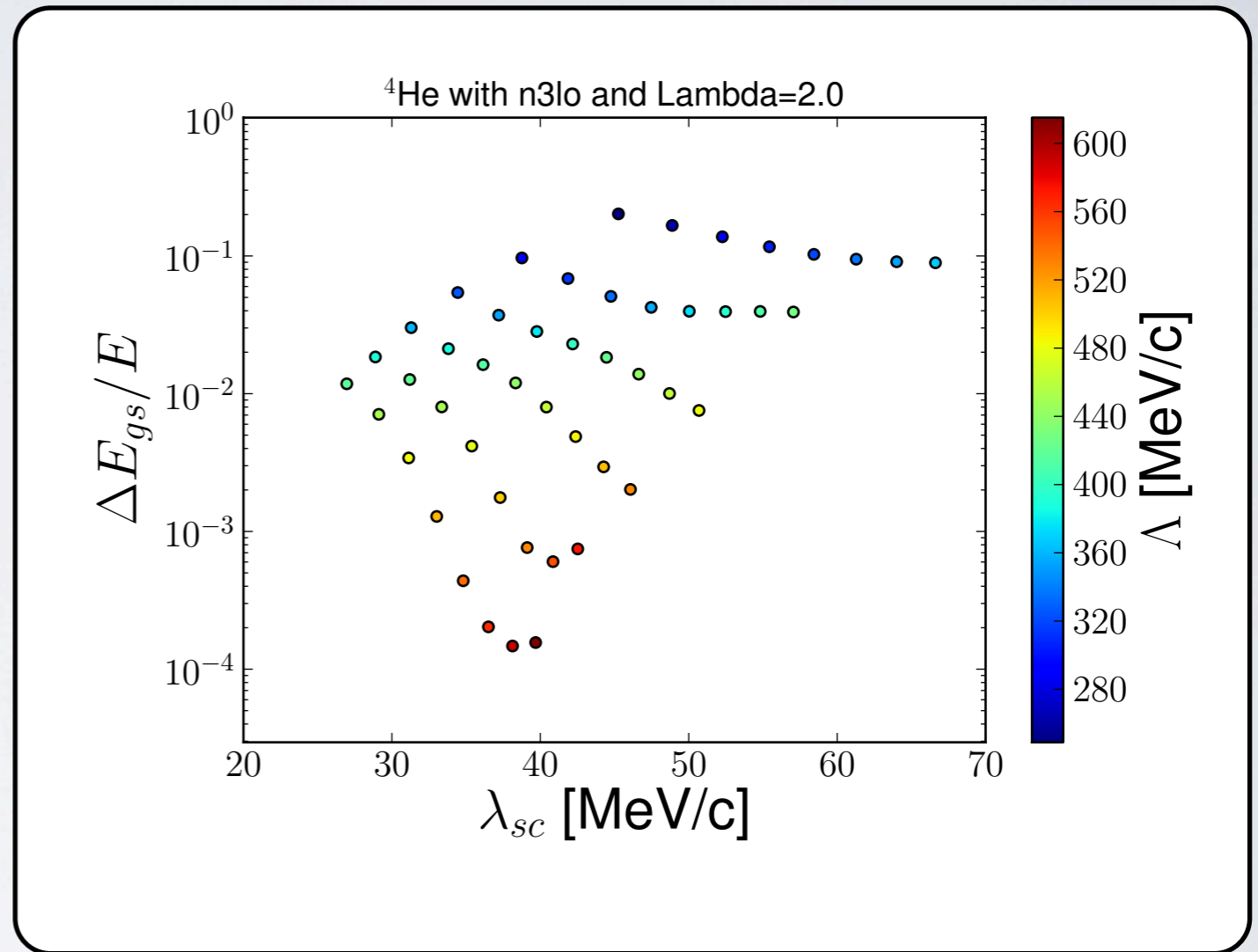
- ❖ Plot $\Delta E/E_{\text{conv}}$ as a function of $\lambda_{\text{sc}} \equiv \sqrt{m\hbar\Omega/(N + 3/2)}$ and $\Lambda \equiv \sqrt{m\hbar\Omega(N + 3/2)}$
- ❖ Universal dependence on λ_{sc} over wide range of $\Delta E/E_{\text{conv}}$.
- ❖ Fit shows exponential in $1 / \lambda_{\text{sc}}$
- ❖ Plateaus to the left from UV corrections



S. Coon et al., arXiv:1205.3230.

Switching to IR and UV cutoffs as variables

- ❖ Plot $\Delta E/E_{\text{conv}}$ as a function of $\lambda_{\text{sc}} \equiv \sqrt{m\hbar\Omega/(N + 3/2)}$ and $\Lambda \equiv \sqrt{m\hbar\Omega(N + 3/2)}$
- ❖ Universal dependence on λ_{sc} over wide range of $\Delta E/E_{\text{conv}}$.
- ❖ Fit shows exponential in $1 / \lambda_{\text{sc}}$
- ❖ Plateaus to the left from UV corrections



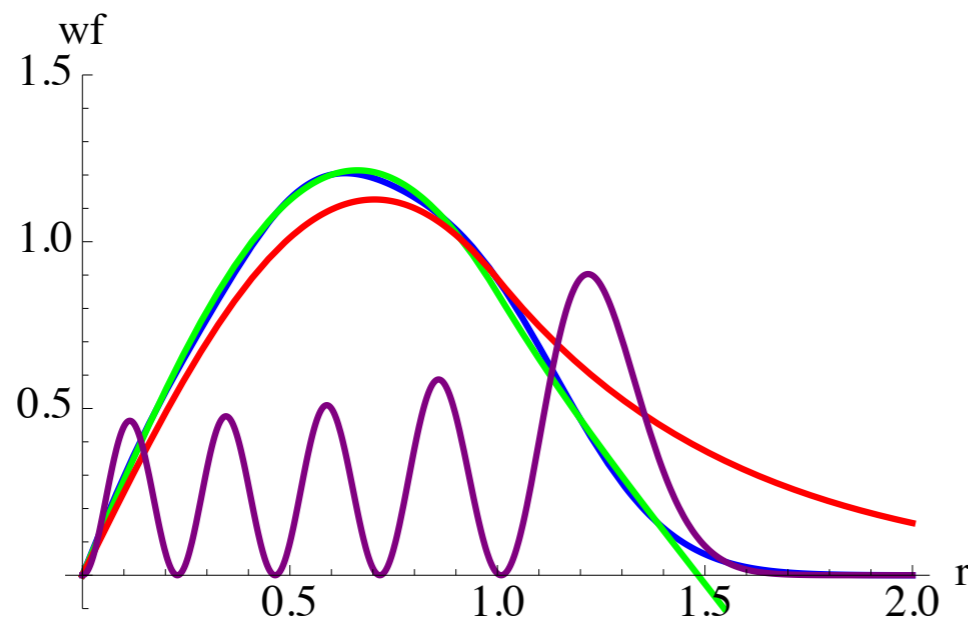
Our calculations
- not fixed Λ but color mapped

Nature and form of IR and UV corrections

Truncated basis cuts off s.p. wave functions

- First estimate of cutoffs: $\frac{1}{2} m \Omega^2 r_{\max}^2 = \frac{1}{2m} p_{\max}^2 = (N + 3/2) \hbar \Omega$
 $\implies \Lambda_{UV} = \sqrt{2(N + 3/2) \hbar} / b$ and $L_0 = \sqrt{2(N + 3/2) b}$
with $b = \sqrt{\hbar / m \Omega}$ (note $\sqrt{2}$'s)
- Improved estimate for L from intercept of tangent at $r = L_0$:

$$L_{NLO} \approx L_0 + 0.54437 b (L_0/b)^{-1/3}$$



- Square-well wave functions with mass $m = 1$, radius $R = 1$, and depth $V_0 = 4$
- Exact (red) is compared to HO with $\hbar \Omega = 10$ and $N = 8$ (blue) and to boundary condition at $r = L$ (green) and to $n = 4$ wf squared (purple)

$$E_{\text{exact}} = -1.51, E_{\text{HO}} = -1.23, E_L = -1.14 \text{ [L improved]}$$

R.J. Furnstahl, talk at this program, 2012-10-10

R.J. Furnstahl et al., Phys. Rev. C 86(2012)031301R.

Correction for energy

Linear energy method to estimate corrections [Djajaputra]

- Let $u_E(r)$ be the radial solution regular at $r = 0$ with energy E , then

$$u_L(r) \equiv u_{E_L}(r) \approx u_\infty(r) + \Delta E_L \left. \frac{du_E(r)}{dE} \right|_{E_\infty} \quad \text{where } E_L = E_\infty + \Delta E_L$$

$$\text{So } u_L(L) = 0 \implies \Delta E_L \approx -u_\infty(L) \left(\left. \frac{du_E(L)}{dE} \right|_{E_\infty} \right)^{-1}$$

- Now $u_E(r) \xrightarrow{r \gg R} A_E(e^{-k_E r} + \alpha_E e^{+k_E r})$ with $u_\infty(r) \xrightarrow{r \gg R} A_\infty e^{-k_\infty r}$ and k_∞ from nucleon separation energy $S = \frac{\hbar^2 k_\infty^2}{2m}$
- Take the derivative and evaluate at $E = E_\infty$:

$$\left. \frac{du_E(r)}{dE} \right|_{E_\infty} = +A_\infty \left. \frac{d\alpha_E}{dE} \right|_{E_\infty} e^{+k_\infty r} + \mathcal{O}(e^{-k_\infty r})$$

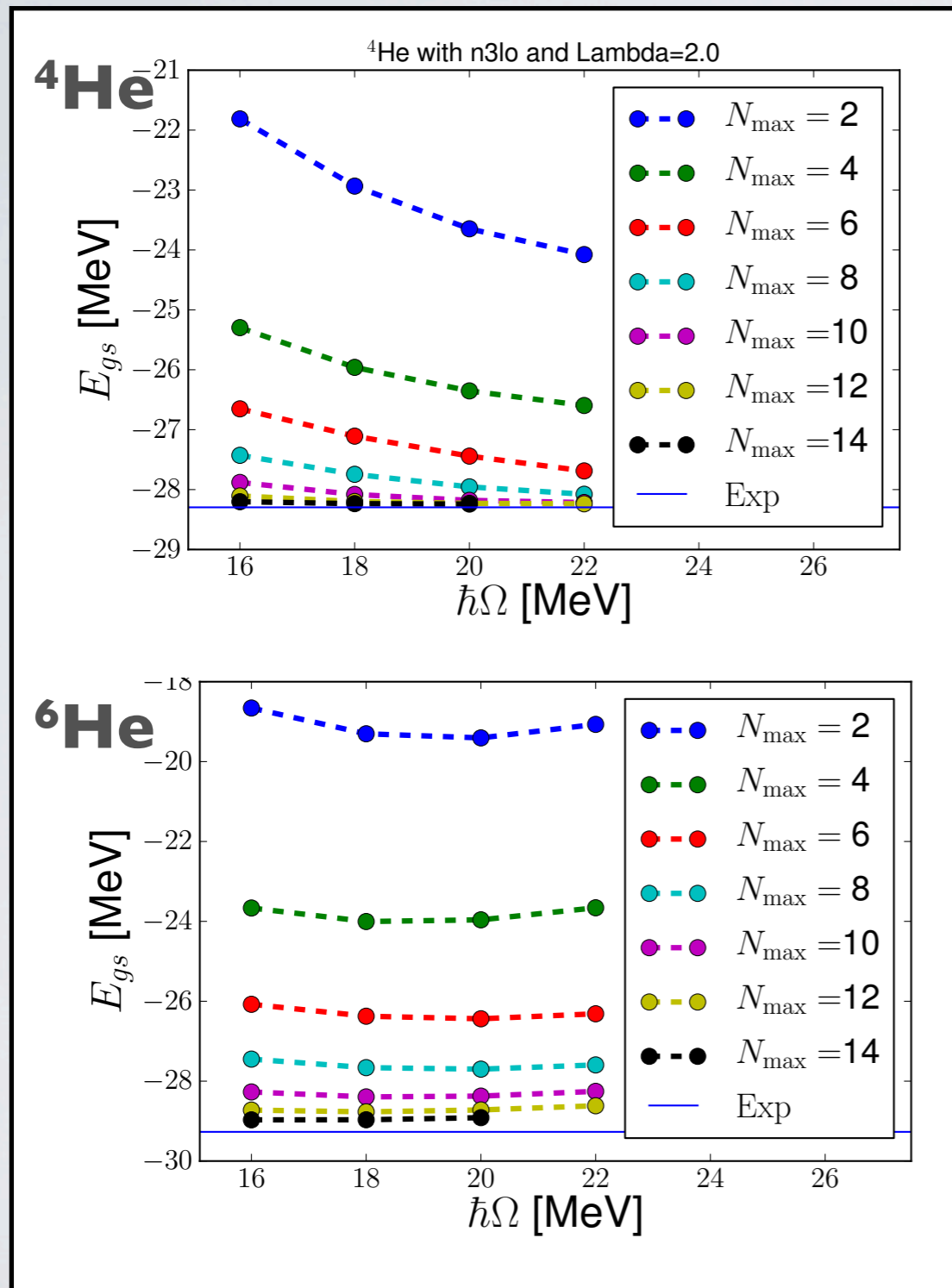
Substituting at $r = L$, we obtain our correction formula to fit:

$$\Delta E_L \approx - \left[\left. \frac{d\alpha_E}{dE} \right|_{E_\infty} \right]^{-1} e^{-2k_\infty L} + \mathcal{O}(e^{-4k_\infty L}) \implies E_L = E_\infty + a_0 e^{-2k_\infty L}$$

R.J. Furnstahl, talk at this program, 2012-10-10

R.J. Furnstahl et al., Phys. Rev. C 86(2012)031301R.

NCSM example: Energy convergence



HO basis cutoff scales

$$\Lambda_{\text{UV}} = \sqrt{2(N + 3/2)}\hbar/b$$

$$L_{\text{IR}} = \sqrt{2(N + 3/2)}b$$

$$L \approx L_{\text{IR}} + 0.544b(L_{\text{IR}}/b)^{-1/3}$$

Extrapolations from finite HO basis

• R.J. Furnstahl et al., Phys. Rev. C 86(2012)031301R

Correction to the energy due to finite HO space

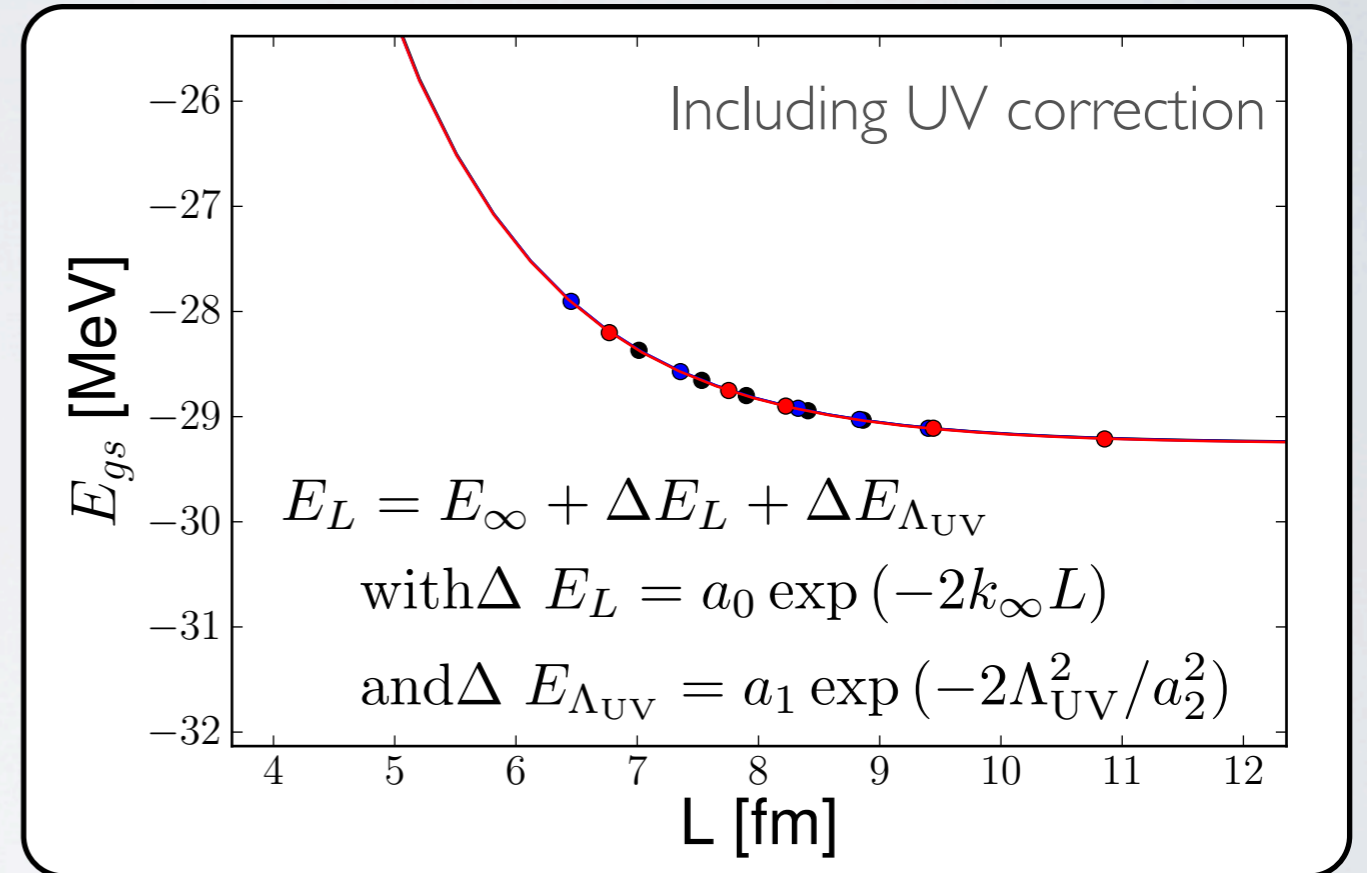
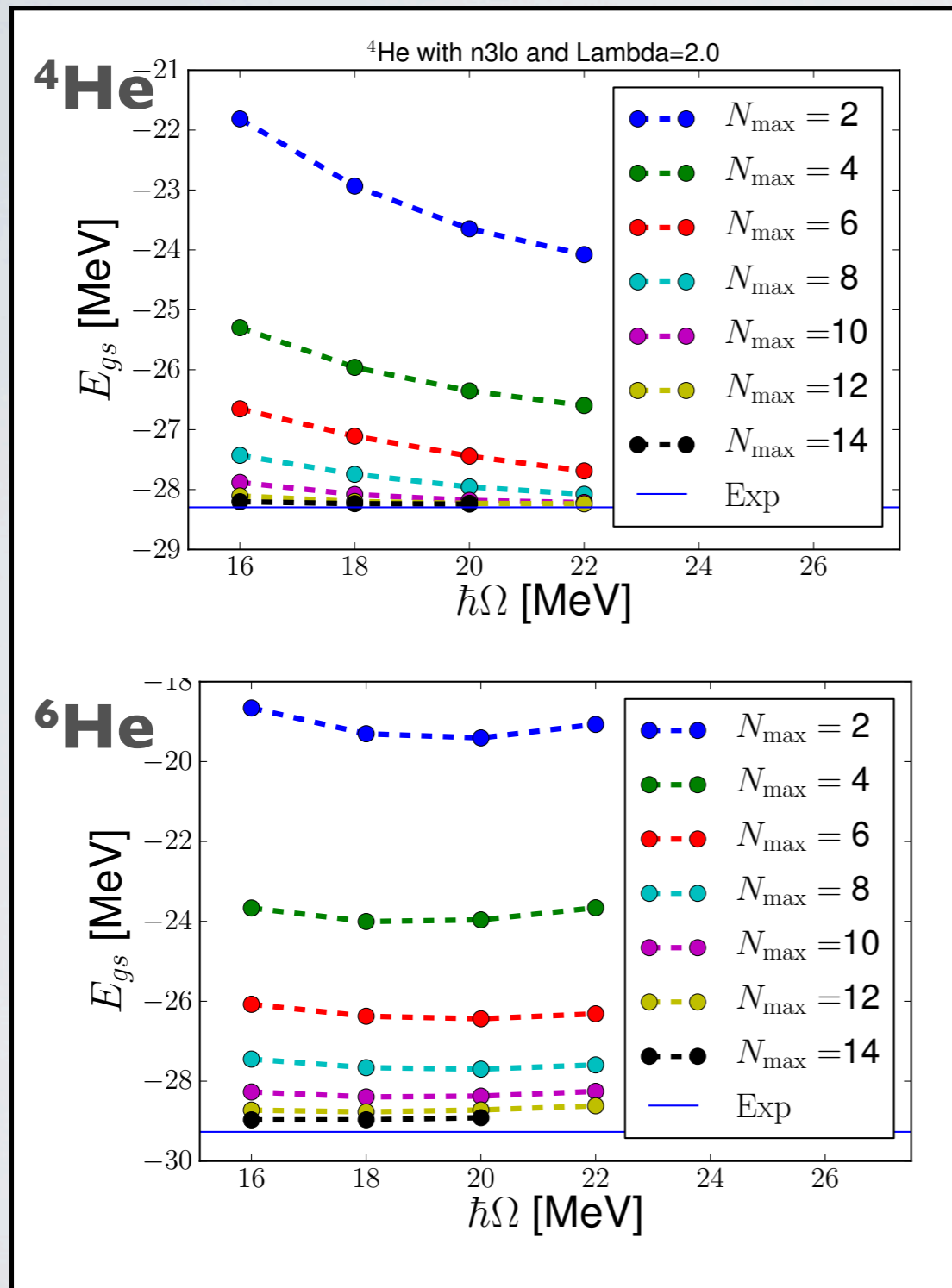
$$E_L = E_\infty + \Delta E_L$$

$$\text{with } \Delta E_L = a_0 \exp(-2k_\infty L)$$

NCSM example: Energy convergence

Binding energies

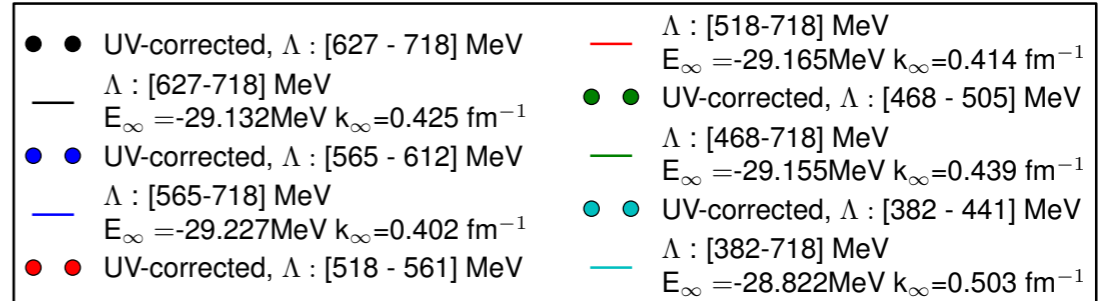
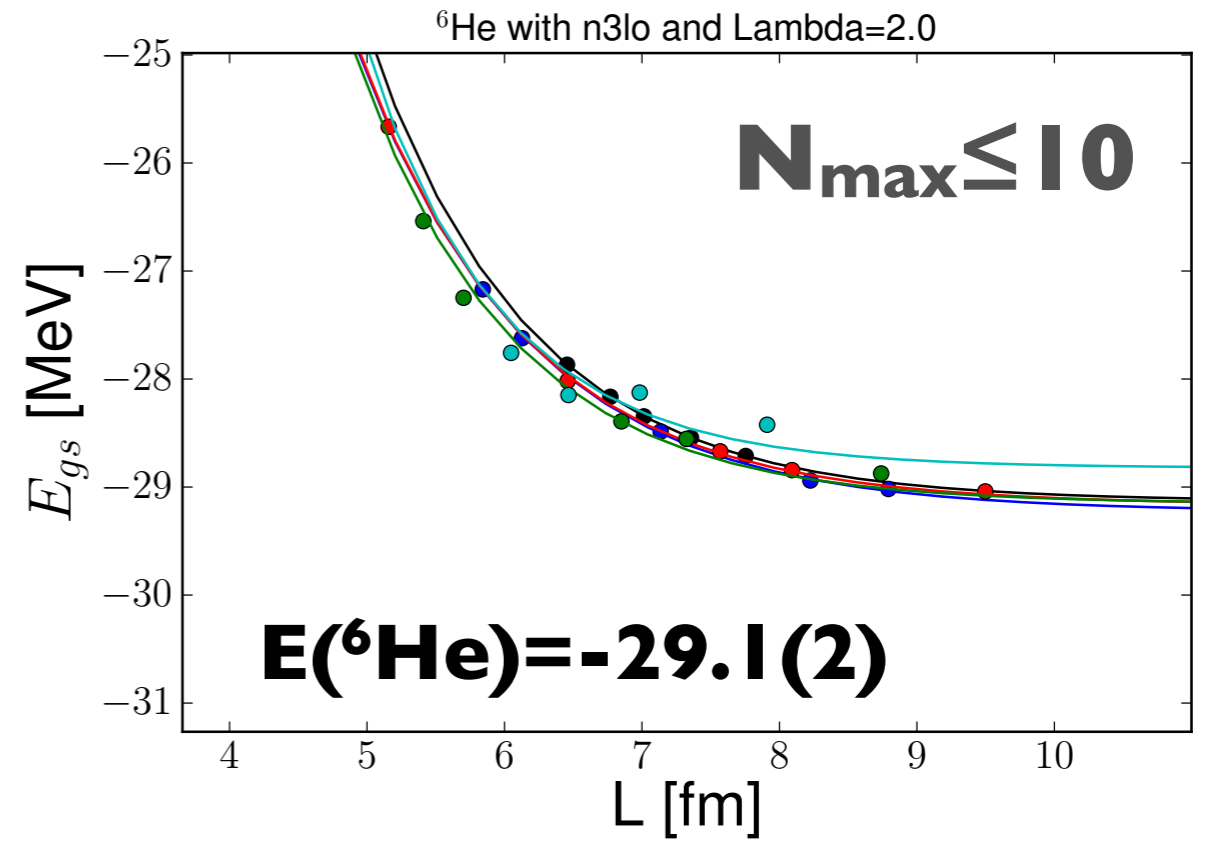
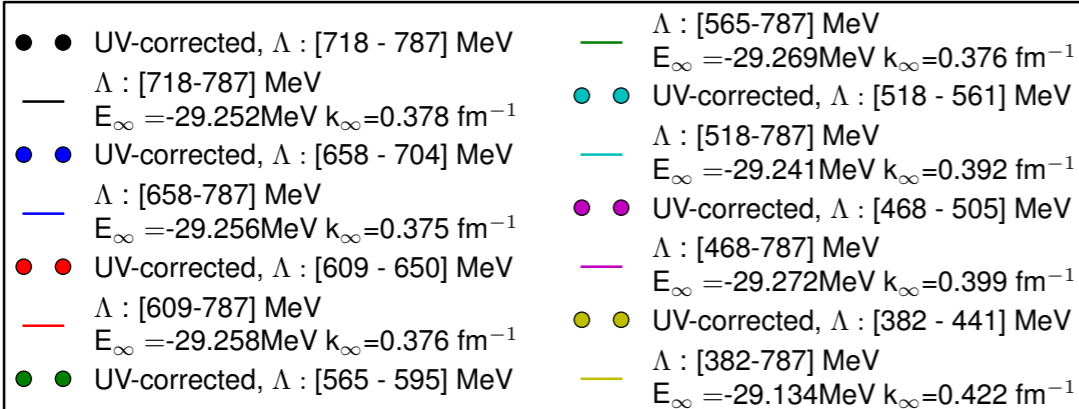
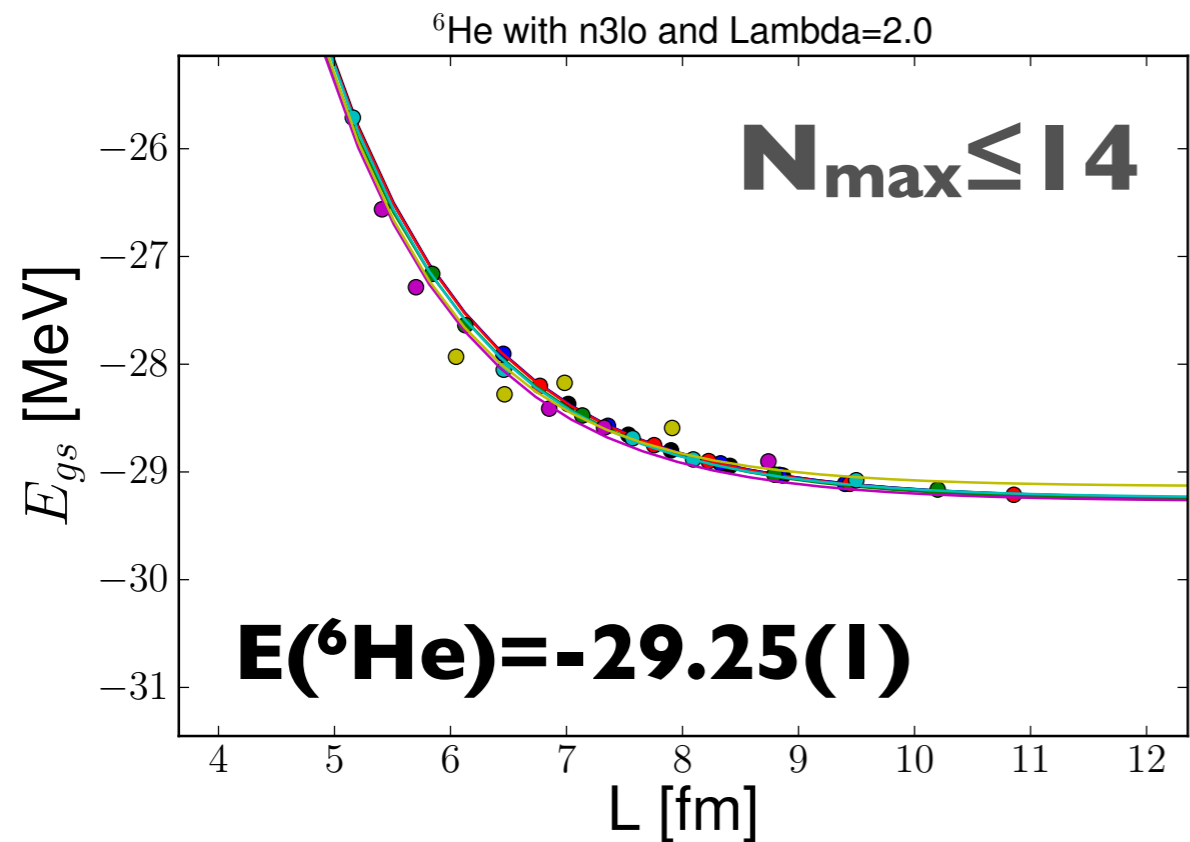
$N^3\text{LO}$, SRG (NN only, $\Lambda = 2.0 \text{ fm}^{-1}$)



$E(^6\text{He})$	-29.25(1) MeV
S_{2n}	1.01(1) MeV

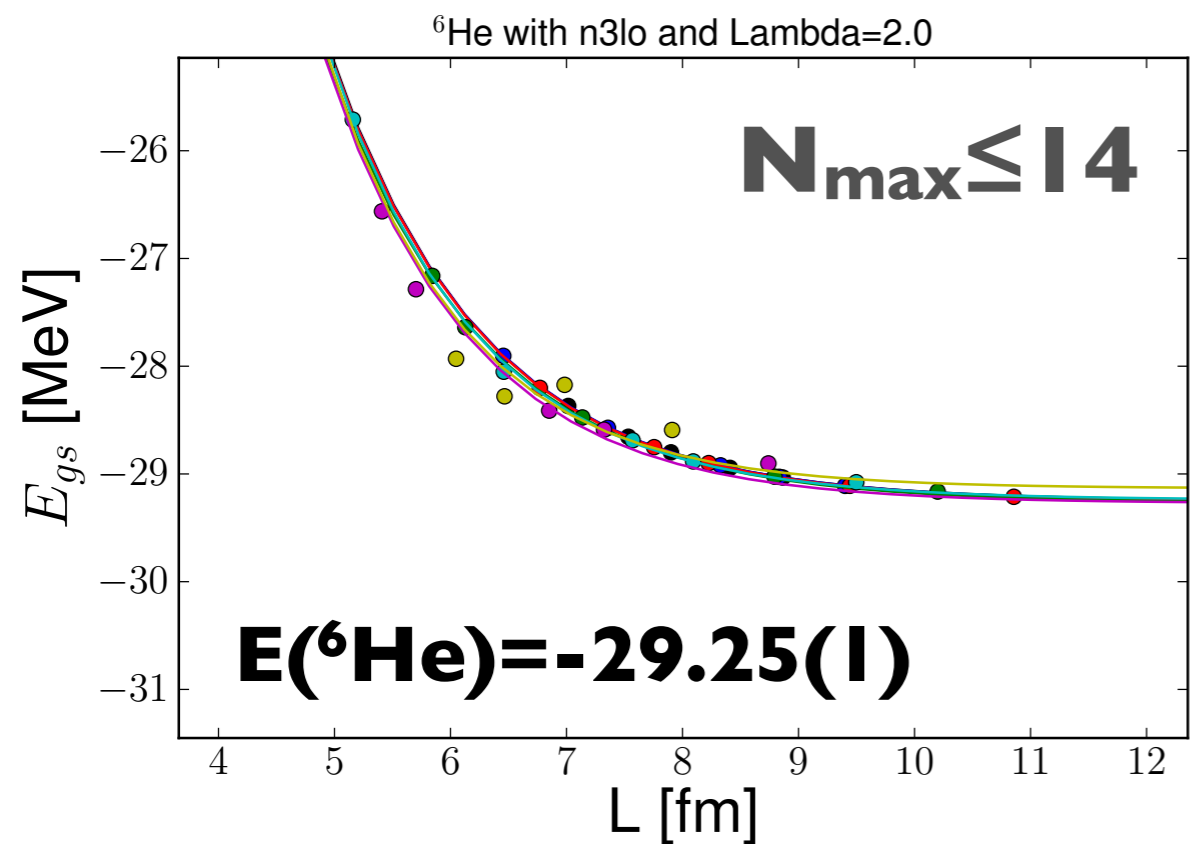
NCSM example: Energy convergence

$N^3\text{LO}$, SRG (NN only, $\Lambda = 2.0 \text{ fm}^{-1}$)

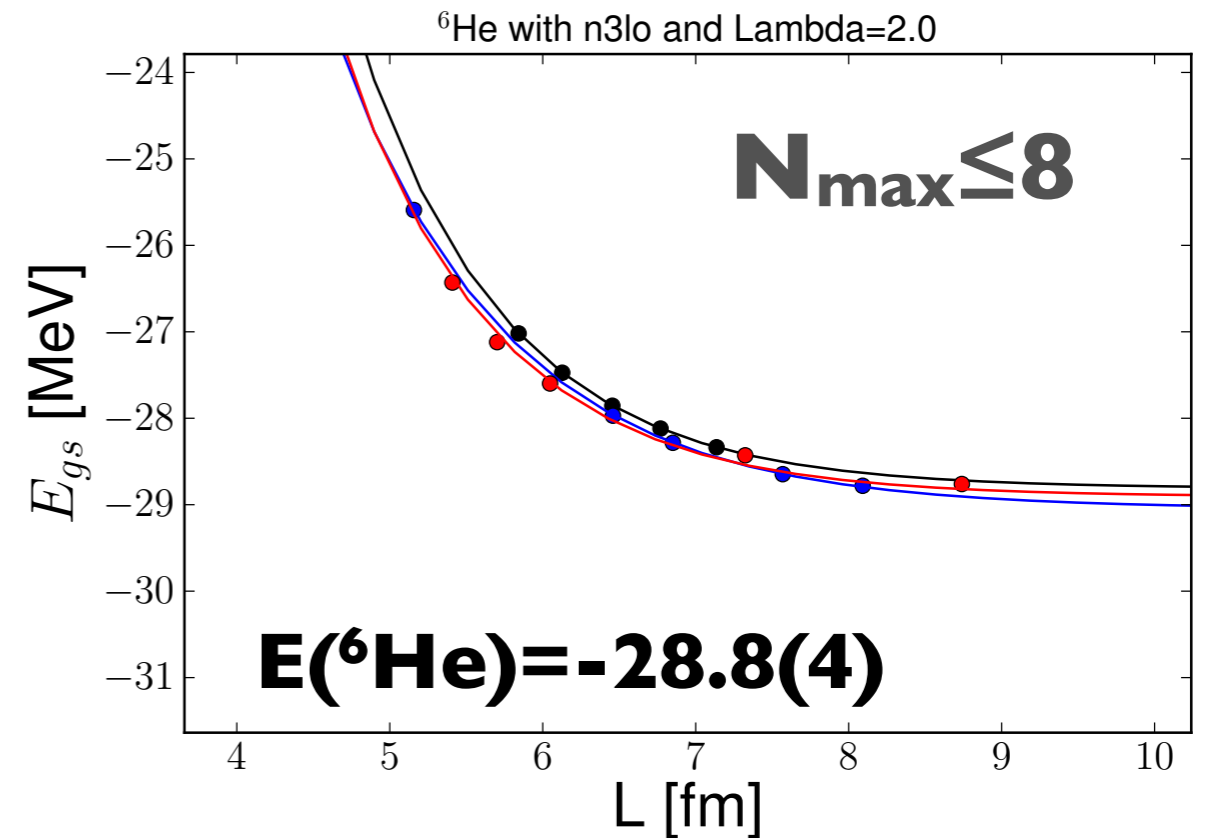


NCSM example: Energy convergence

$N^3\text{LO}$, SRG (NN only, $\Lambda = 2.0 \text{ fm}^{-1}$)



- | | |
|---|---|
| ● ● UV-corrected, Λ : [718 - 787] MeV | — Λ : [565-787] MeV |
| — $E_{\infty} = -29.252\text{MeV}$ $k_{\infty} = 0.378 \text{ fm}^{-1}$ | ● ● UV-corrected, Λ : [518 - 561] MeV |
| ● ● UV-corrected, Λ : [658 - 704] MeV | — Λ : [518-787] MeV |
| — $E_{\infty} = -29.256\text{MeV}$ $k_{\infty} = 0.375 \text{ fm}^{-1}$ | — $E_{\infty} = -29.241\text{MeV}$ $k_{\infty} = 0.392 \text{ fm}^{-1}$ |
| ● ● UV-corrected, Λ : [609 - 650] MeV | ● ● UV-corrected, Λ : [468 - 505] MeV |
| — $E_{\infty} = -29.258\text{MeV}$ $k_{\infty} = 0.376 \text{ fm}^{-1}$ | — Λ : [468-787] MeV |
| ● ● UV-corrected, Λ : [565 - 595] MeV | — $E_{\infty} = -29.272\text{MeV}$ $k_{\infty} = 0.399 \text{ fm}^{-1}$ |
| | ● ● UV-corrected, Λ : [382 - 441] MeV |
| | — Λ : [382-787] MeV |
| | — $E_{\infty} = -29.134\text{MeV}$ $k_{\infty} = 0.422 \text{ fm}^{-1}$ |



- | | |
|---|---|
| ● ● UV-corrected, Λ : [565 - 658] MeV | — Λ : [505-658] MeV |
| — $E_{\infty} = -28.811\text{MeV}$ $k_{\infty} = 0.513 \text{ fm}^{-1}$ | — $E_{\infty} = -29.048\text{MeV}$ $k_{\infty} = 0.446 \text{ fm}^{-1}$ |
| ● ● UV-corrected, Λ : [505 - 561] MeV | ● ● UV-corrected, Λ : [441 - 494] MeV |
| | — Λ : [441-658] MeV |
| | — $E_{\infty} = -28.908\text{MeV}$ $k_{\infty} = 0.503 \text{ fm}^{-1}$ |

Correction for radius

Correction for radius (or other long-distance operators)

- Use $u_L(r) \approx u_\infty(r) + \Delta E_L \left. \frac{du_E(r)}{dE} \right|_{E_\infty}$ to evaluate

$$\Delta \langle r^2 \rangle_L = \langle r^2 \rangle_L - \langle r^2 \rangle_\infty = \frac{\int_0^L |u_L(r)|^2 r^2 dr}{\int_0^L |u_L(r)|^2 dr} - \frac{\int_0^\infty |u_\infty(r)|^2 r^2 dr}{\int_0^\infty |u_\infty(r)|^2 dr}$$

- For leading L dependence, use $u_\infty(r) \rightarrow A_\infty e^{-k_\infty r}$ and

$$\left. \frac{du_E(r)}{dE} \right|_{E_\infty} \approx -\frac{A_\infty}{\Delta E_L} e^{-2k_\infty L} e^{+k_\infty r} \implies \Delta \langle r^2 \rangle_L \propto \langle r^2 \rangle_\infty (2k_\infty L)^3 e^{-2k_\infty L}$$

- The NLO correction scales as $(2k_\infty L) \exp(-2k_\infty L)$, so

$$\langle r^2 \rangle_L \approx \langle r^2 \rangle_\infty [1 - (c_0 \beta^3 + c_1 \beta) e^{-\beta}] \quad \text{with } \beta \equiv 2k_\infty L$$

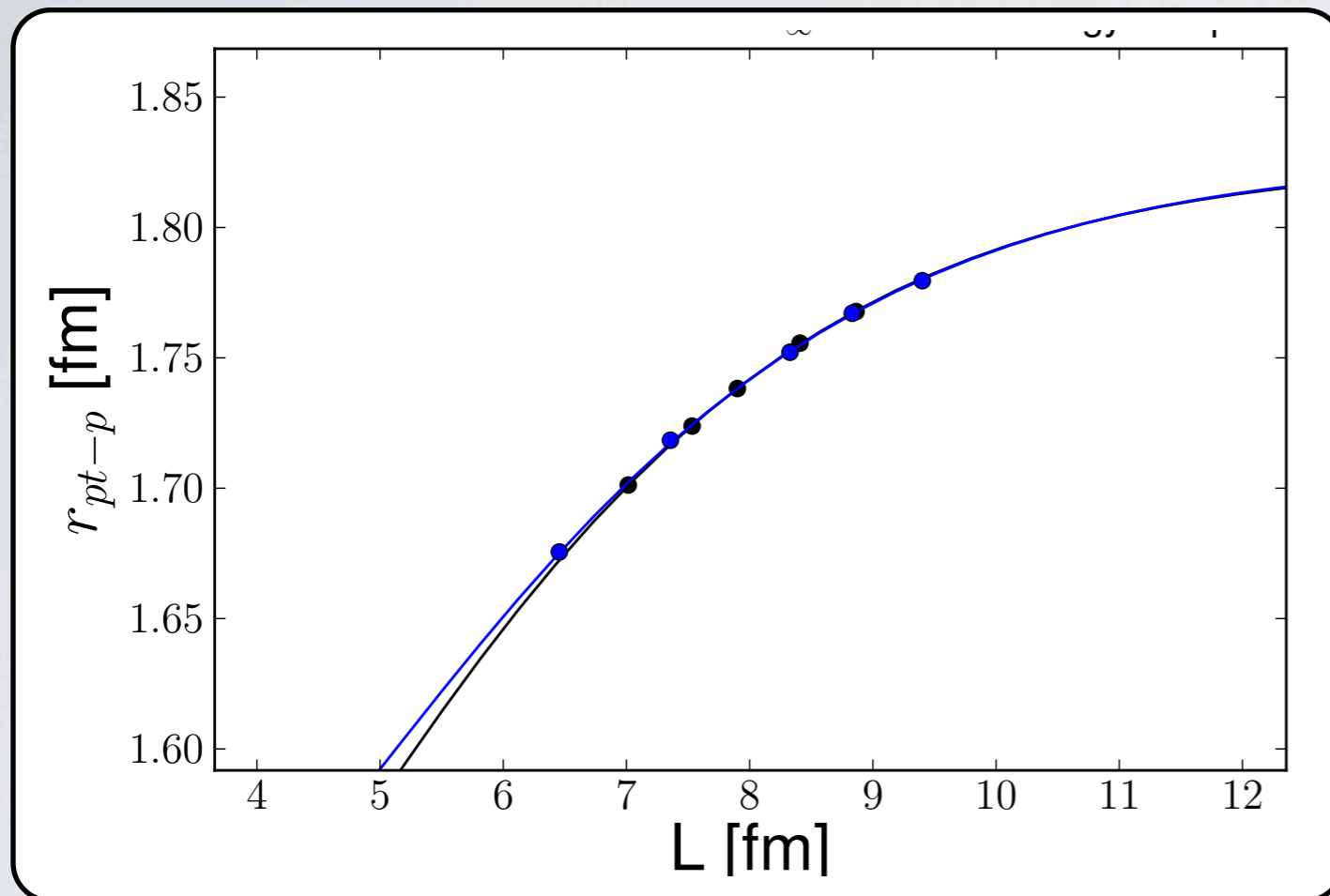
- $\langle r^2 \rangle_\infty$, c_0 , and c_1 are fit parameters while k_∞ from energy fit
- Valid in the asymptotic regime where $\beta = 2k_\infty L \gtrsim 3$
- Both E and r corrections apply to A -body system in lab coordinates

R.J. Furnstahl, talk at this program, 2012-10-10

R.J. Furnstahl et al., Phys. Rev. C 86(2012)031301R.

${}^6\text{He}$: Point-Proton Radius

${}^6\text{He}$ point-proton radius

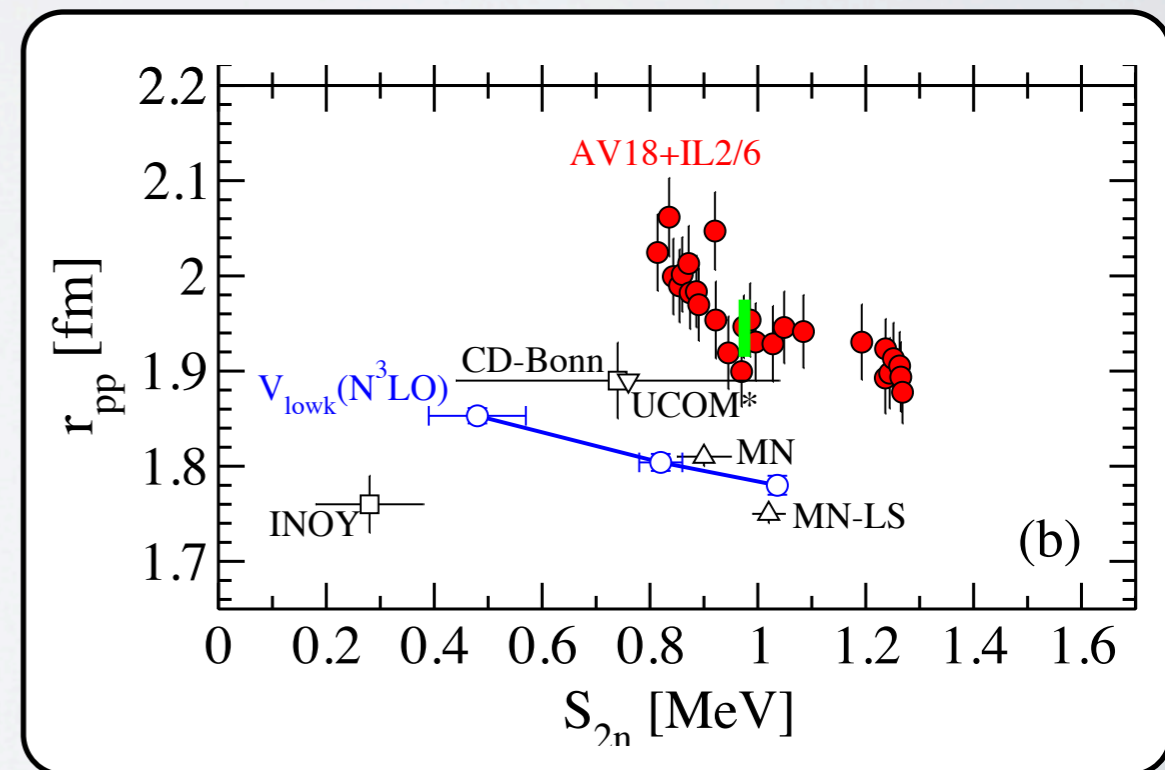


$$\langle r^2 \rangle_L \approx \langle r^2 \rangle_\infty [1 - (c_0 \beta^3 + c_1 \beta) e^{-\beta}]$$

with $\beta \equiv 2k_\infty L$

From: R.J. Furnstahl et al., Phys. Rev. C 86(2012)031301R.

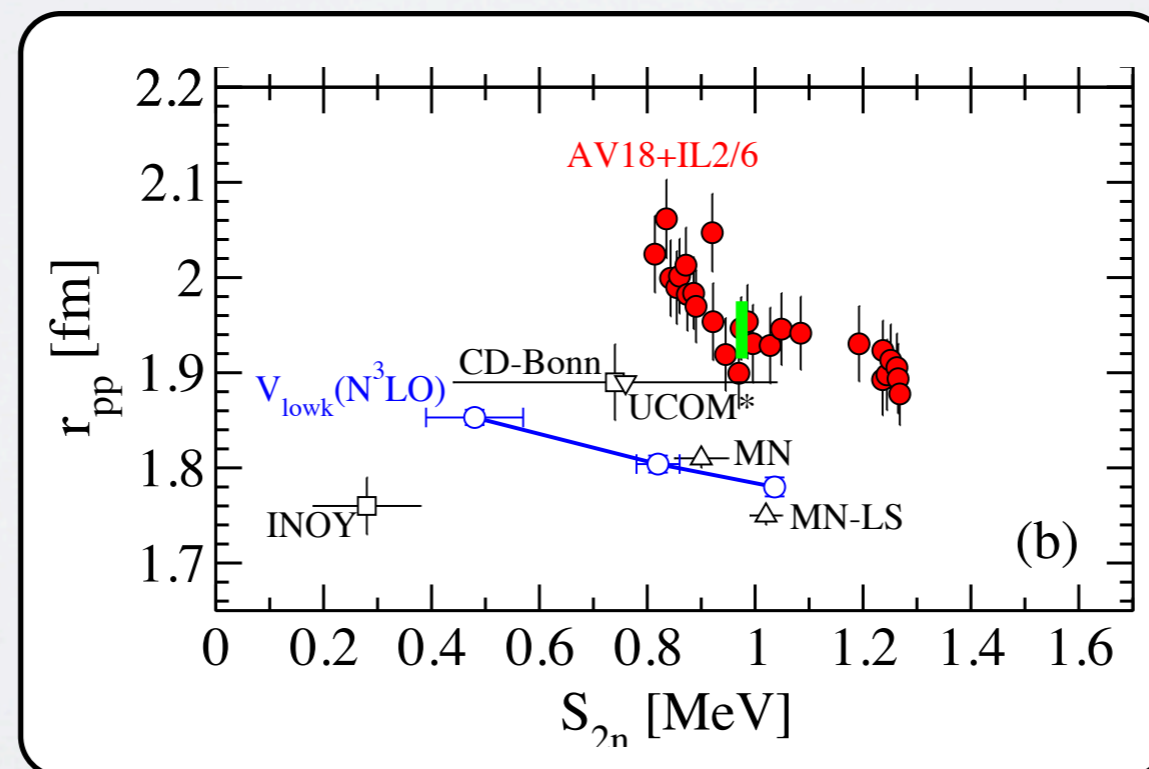
Ref.	$r_{\text{pt-p}}({}^6\text{He})$
Exp	1.938(23)
NCSM: I-N3LO ($\Lambda = 2 \text{ fm}^{-1}$)	1.83(1)
HH (S. Bacca et al): I-N3LO (LS+ V_{lowk} , 2 fm^{-1})	1.804(9)



C. Forssén, INT, Oct. 31, 2012

${}^6\text{He}$: Point-Proton Radius

Ref.	$r_{\text{pt-p}}({}^6\text{He})$ [fm]	$S_{2n}({}^6\text{He})$ [fm]
Exp	1.938(23)	0.97
NCSM: I-N3LO ($\Lambda = 1.8 \text{ fm}^{-1}$)	1.81(1)	1.17(4)
NCSM: I-N3LO ($\Lambda = 2.0 \text{ fm}^{-1}$)	1.83(1)	1.01(1)
NCSM: I-N3LO ($\Lambda = 2.2 \text{ fm}^{-1}$)	1.85(3)	0.82(2)

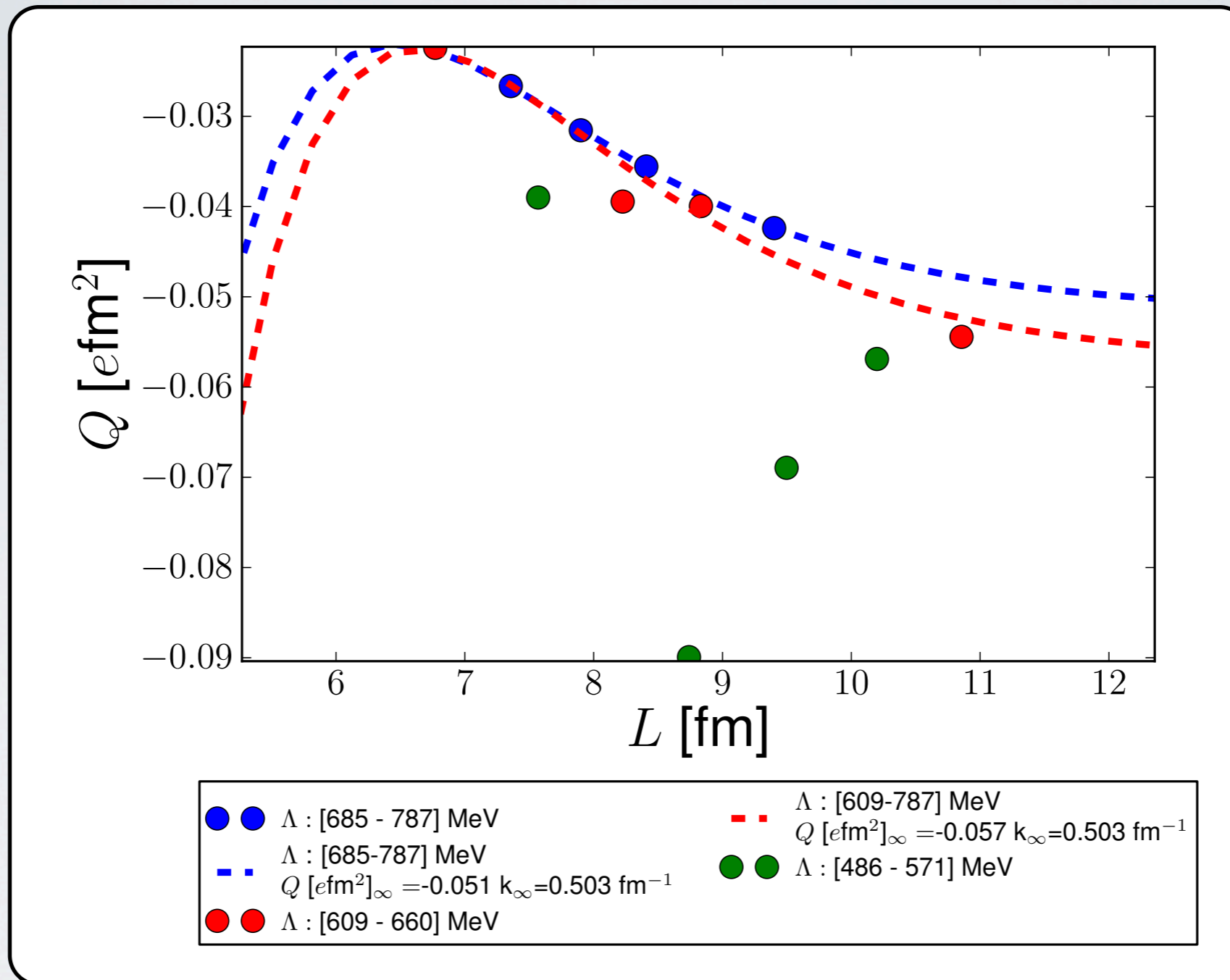


Unsettled questions for the IR extrapolation

Selected from list by R.J. Furnstahl, talk at this program, 2012-10-10

- ❖ What is the optimal definition of L ?
- ❖ How to make credible error estimates?
- ❖ Does the interaction matter?
 - ▶ The IR corrections are independent of the potential
 - ▶ Softer interactions mean more complete UV convergence, so larger region with IR corrections only.
- ❖ How well does extrapolation work for other operators?

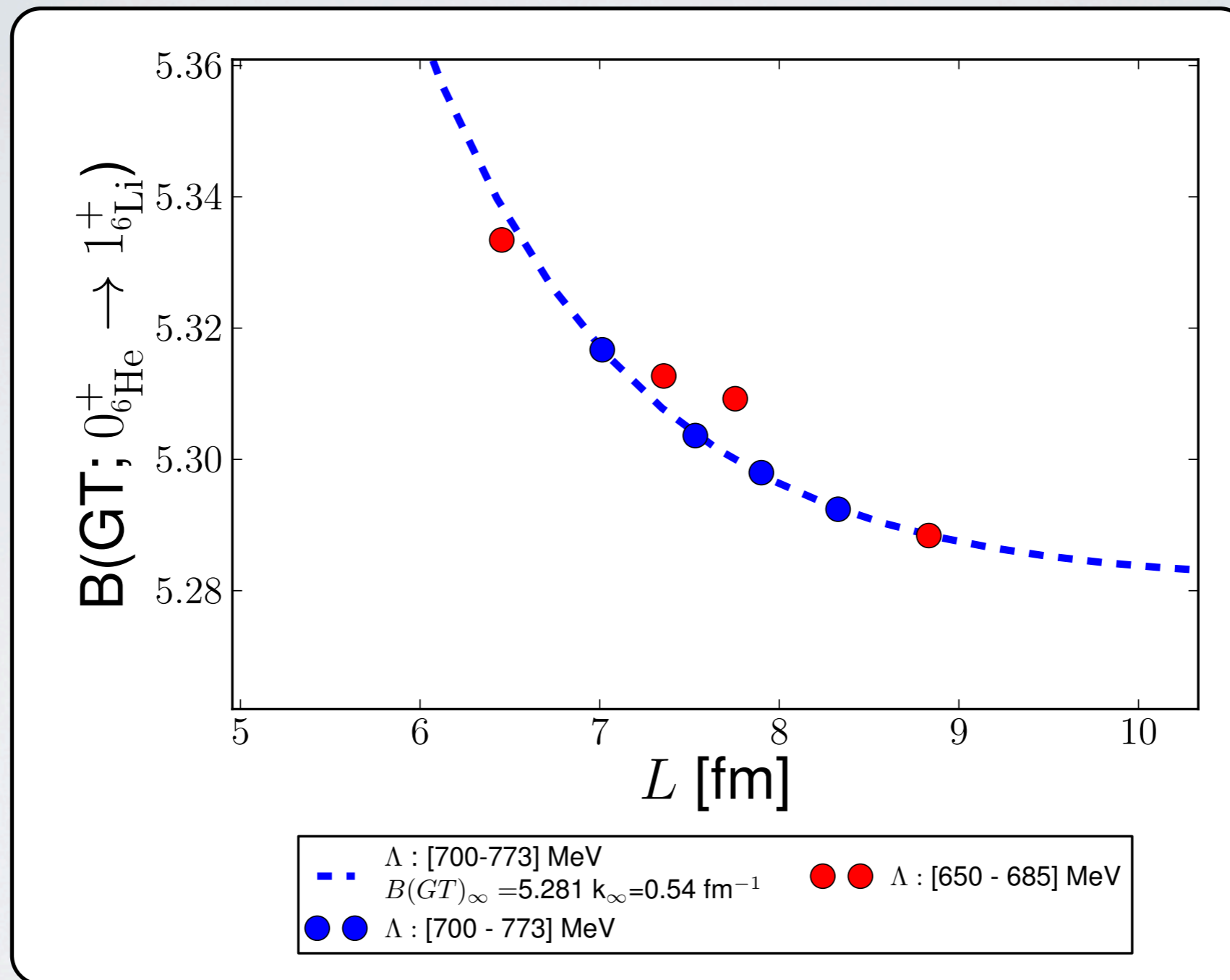
$Q(^6\text{Li}, I^+)$



$$\langle O \rangle_L \approx \langle O \rangle_{\infty} \left[1 - (c_0 \beta^3 + c_1 \beta) e^{-\beta} \right]$$

$$\text{with } \beta \equiv 2k_{\infty} L$$

B(GT): ${}^6\text{He} \rightarrow {}^6\text{Li}$



$$\langle O \rangle_L \approx \langle O \rangle_\infty \left[1 - (c_0 \beta^3 + c_1 \beta) e^{-\beta} \right]$$

$$\text{with } \beta \equiv 2k_\infty L$$

Conclusions - Cutoff scales

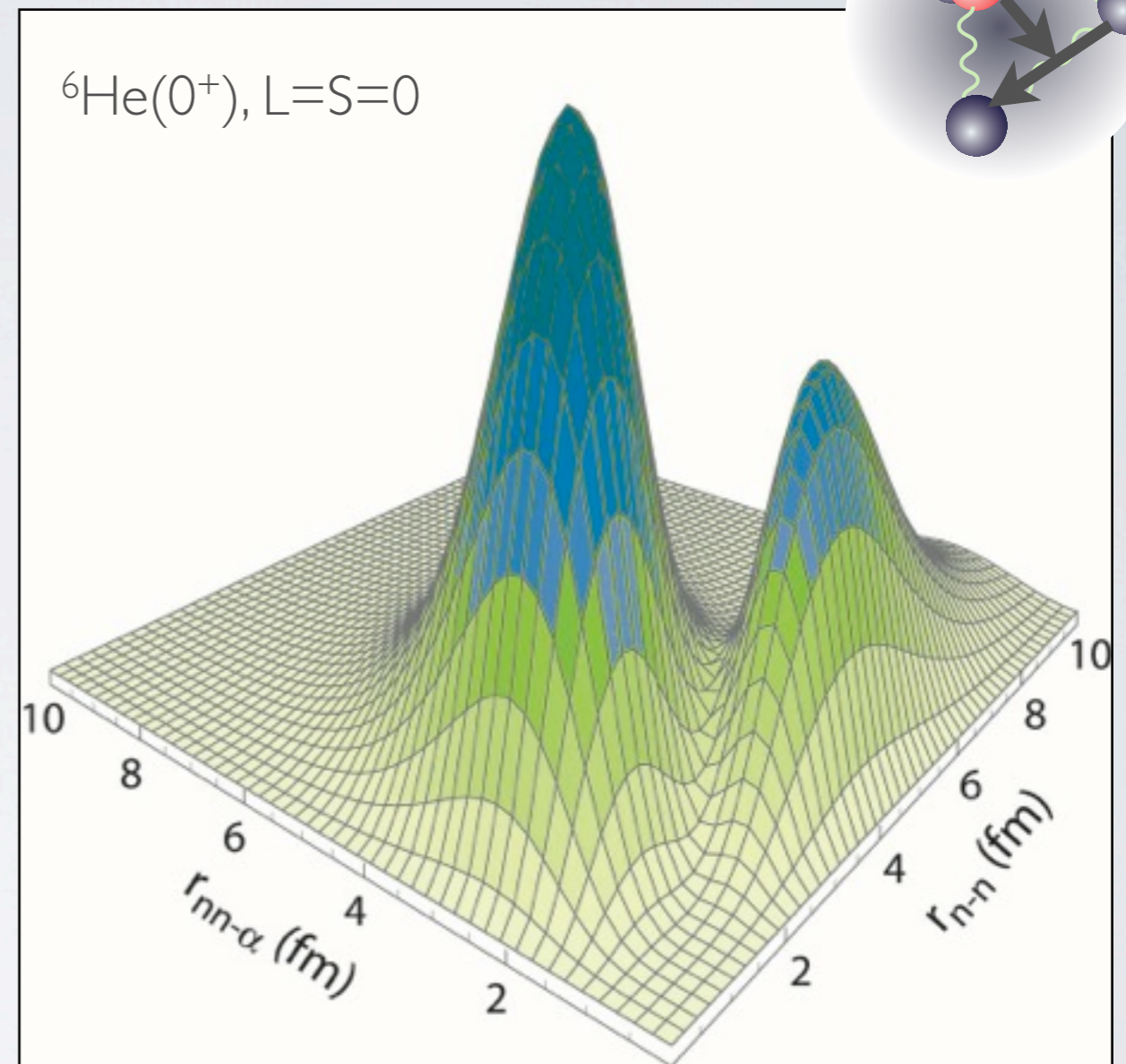
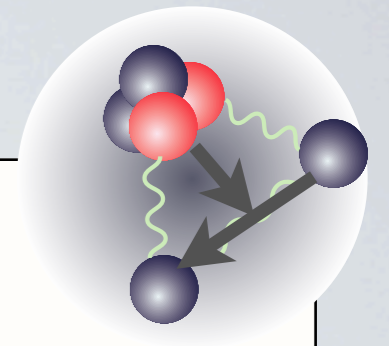
- ❖ Introduction of UV and IR scales - Combination of results from different N_{\max} , $\hbar\Omega$
- ❖ Optimization of run sequence - BUT still need several large N_{\max} computations
- ❖ Prefer UV converged results and perform IR extrapolation
- ❖ Transformation of operators

A Microscopic Description Of Clustering

${}^6\text{He}$ as a three-body system

- ❖ Borromean nucleus
- ❖ HH and CSF three-body models with inert cluster.
 V_{nn} and $V_{n\alpha}$
 - ▶ Core polarization needed
 $r_{n\alpha} = 1.03 r_{n\alpha(\text{free})}$
(cf. three-body force)
 - ▶ Repulsive s-wave potential (“Pauli core”)
 - ▶ HH expansion
K=2 (90%) with L=S=0 (80%)
and L=S=1 (10%)
- ❖ Pauli focusing.

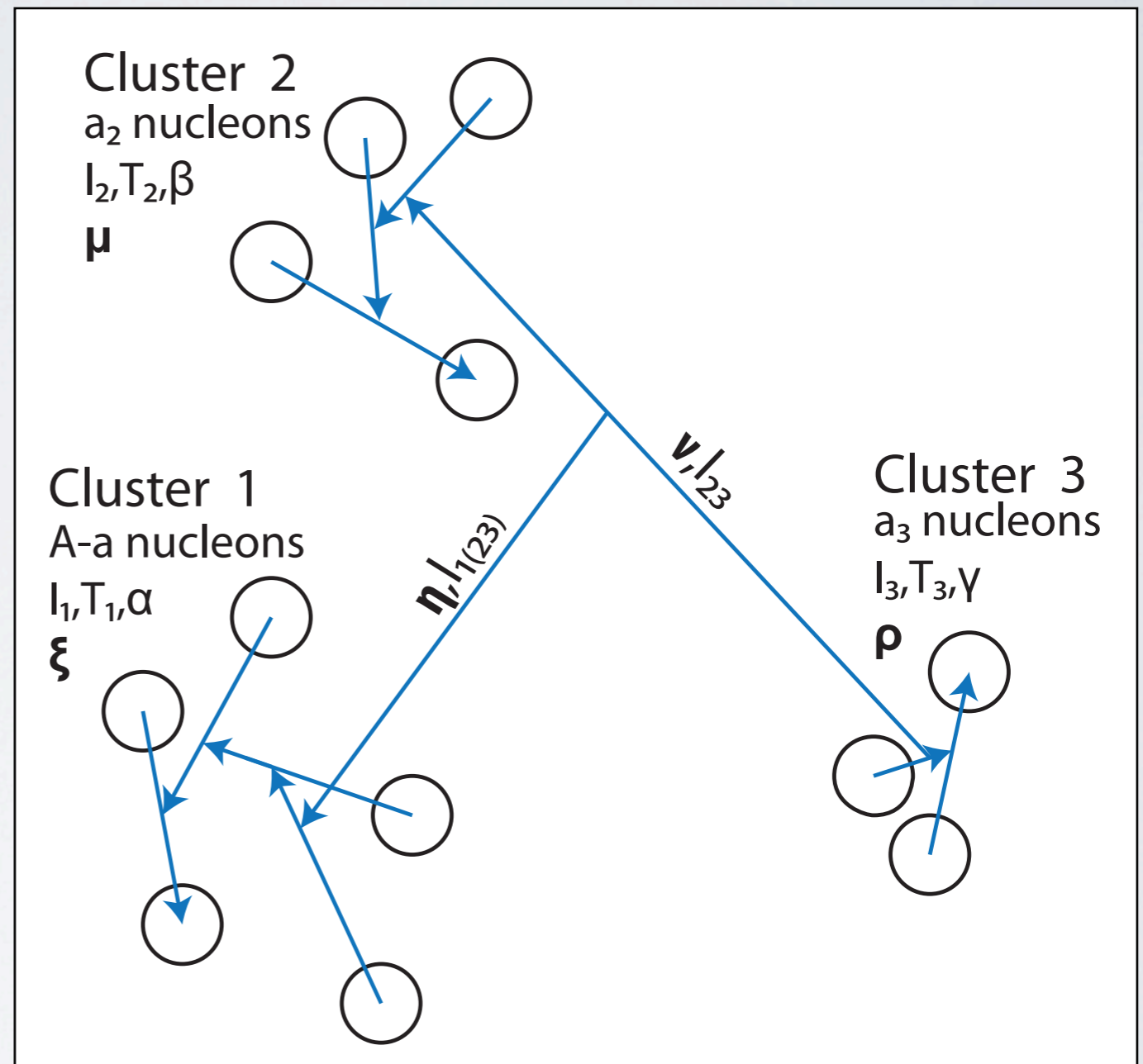
$${}^6\text{He} = {}^4\text{He} + n + n$$



M.V. Zhukov et al.— Phys. Rep. **231**, 151 (1993),

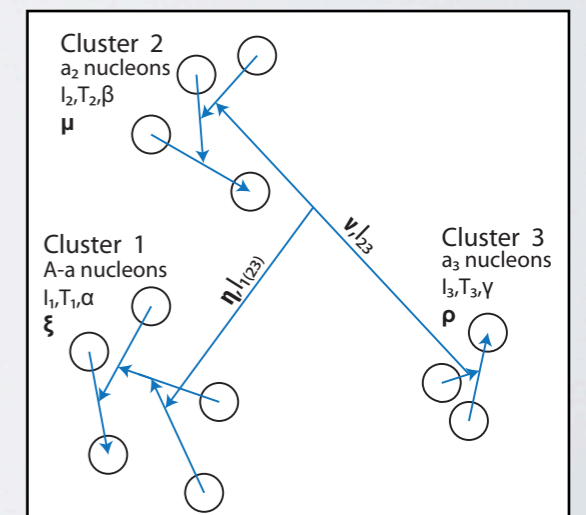
Cluster structures in light nuclei

- ❖ Investigate clustering in NCSM wave functions
- ❖ Preserve translational invariance
- ❖ Harmonic oscillator SD many-body basis
- ❖ Transformation between single-particle and Jacobi coordinates



Three-body cluster overlap functions

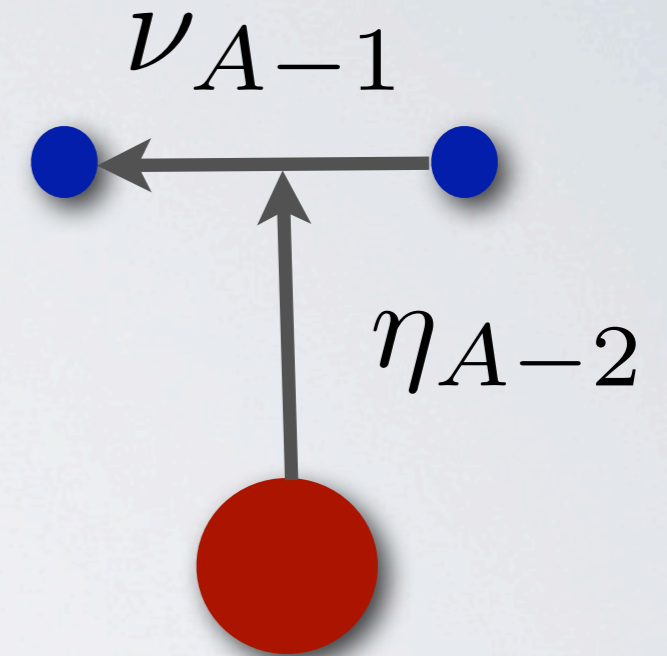
$$\begin{aligned}
 & U_{A-a}^{A\lambda JT} \alpha l_1 T_1, a_2 \beta l_2 T_2, a_3 \gamma l_3 T_3; LS (\eta_{A-a}, \nu_{A-a+1}) \\
 &= \left\langle A\lambda JT \left| \mathcal{A}_{A-a, a_2, a_3} \Phi_{\alpha l_1 T_1, \beta l_2 T_2, \gamma l_3 T_3; LS}^{(A-a, a_2, a_3)JT} : \delta_{\eta_{A-a}}, \delta_{\nu_{A-a+1}} \right. \right\rangle \\
 &= \sum_{n_{1(23)}, n_{23}} R_{n_{1(23)} l_{1(23)}} (\eta_{A-a}) R_{n_{23} l_{23}} (\nu_{A-a+1}) \\
 &\times \sqrt{\frac{A!}{(A-a)! a_2! a_3!}} \left\langle A\lambda JT \left| \Phi_{\alpha l_1 T_1, \beta l_2 T_2, \gamma l_3 T_3; LS}^{(A-a, a_2, a_3)JT} : n_{1(23)} l_{1(23)}, n_{23} l_{23} \right. \right\rangle
 \end{aligned}$$



Overlap function for core+N+N

Start with the **core+N+N** case:

- ❖ Do a couple of coordinate transformations (between relative and s.p.)
- ❖ Do a number of spin re-couplings
- ❖ Integrate over coordinates



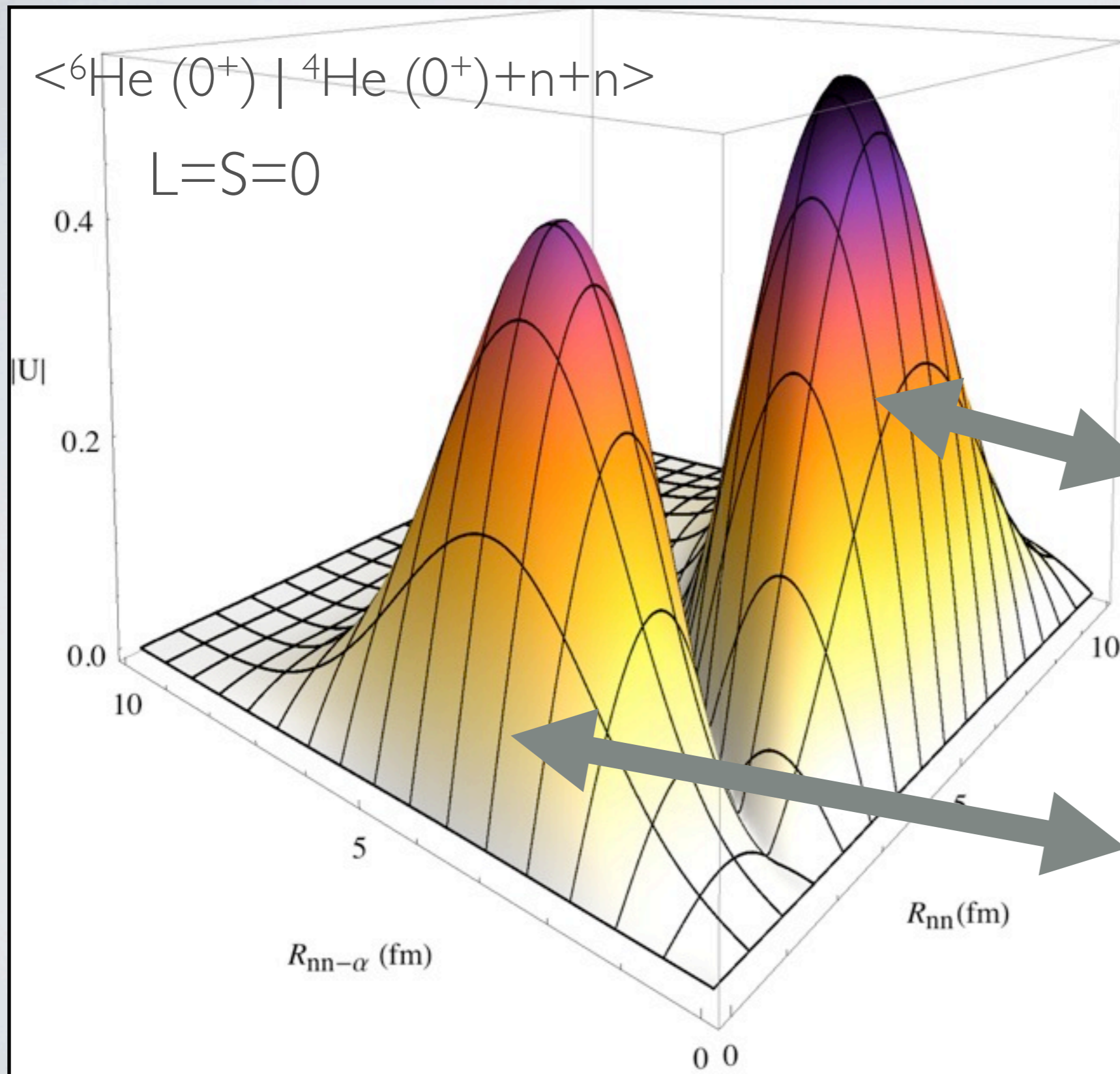
Overlap function for core+N+N

$$\begin{aligned}
 & u_{A-2\alpha l_1 T_1, \frac{1}{2} \frac{1}{2}, \frac{1}{2} \frac{1}{2}; LS}^{A\lambda JT}(\eta_{A-2}, \nu_{A-1}) \\
 &= \sum \frac{R_{n_1(23) l_1(23)}(\eta_{A-2}) R_{n_{23} l_{23}}(\nu_{A-1})}{\langle n_1(23) l_1(23) 00 l_1(23) | 00 n_1(23) l_1(23) l_1(23) \rangle_{\frac{2}{A-2}}} \\
 &\times \langle n_a l_a n_b l_b L | n_1(23) l_1(23) n_{23} l_{23} L \rangle_1 (-1)^{3l_1 + l_{23} + l_{ab} - T_{23} - S + L} \\
 &\times \frac{\hat{L} \hat{S} \hat{I}_{ab}^2 \hat{j}_a \hat{j}_b}{\hat{J} \hat{T}} \begin{Bmatrix} L & l_{23} & l_{ab} \\ l_1 & J & S \end{Bmatrix} \begin{Bmatrix} l_a & l_b & L \\ \frac{1}{2} & \frac{1}{2} & l_{23} \\ j_a & j_b & l_{ab} \end{Bmatrix} \\
 &\times_{SD} \langle A\lambda JT ||| [a_{n_a l_a j_a t_a}^\dagger a_{n_b l_b j_b t_b}^\dagger]^{l_{ab} T_2} ||| (A-2)\alpha l_1 T_1 \rangle_{SD}.
 \end{aligned}$$

D. Sääf and CF, - in preparation

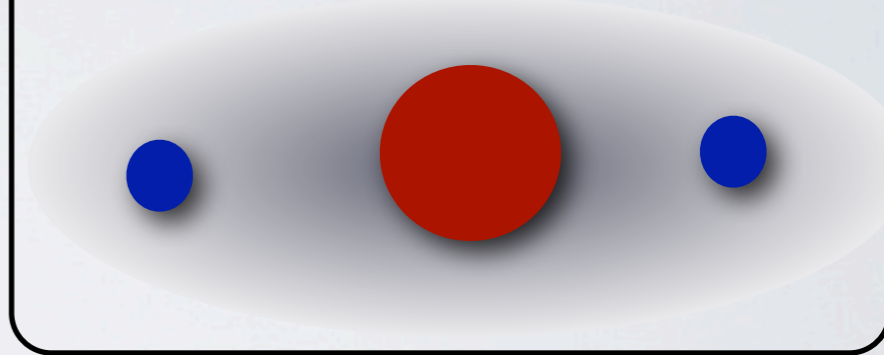
C. Forssén, INT, Oct. 31, 2012

Ab initio $\langle {}^6\text{He} (0^+) | {}^4\text{He} + n + n \rangle$ overlap

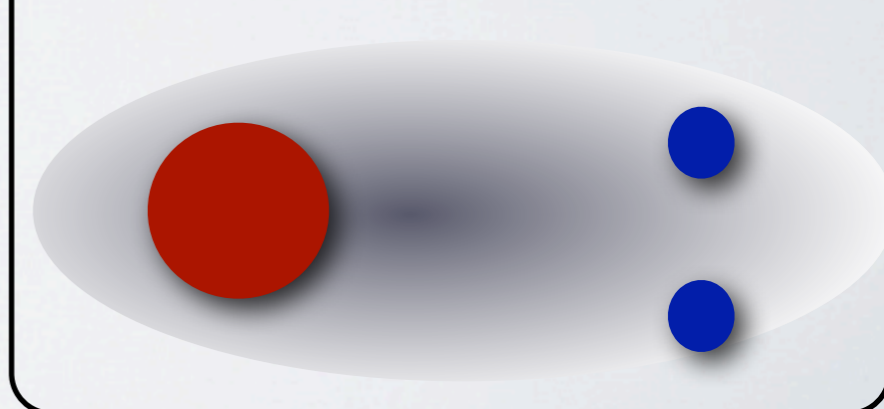


$N^3\text{LO}$, SRG
(NN only, $\Lambda = 2.0 \text{ fm}^{-1}$)

Cigar configuration



Di-neutron configuration



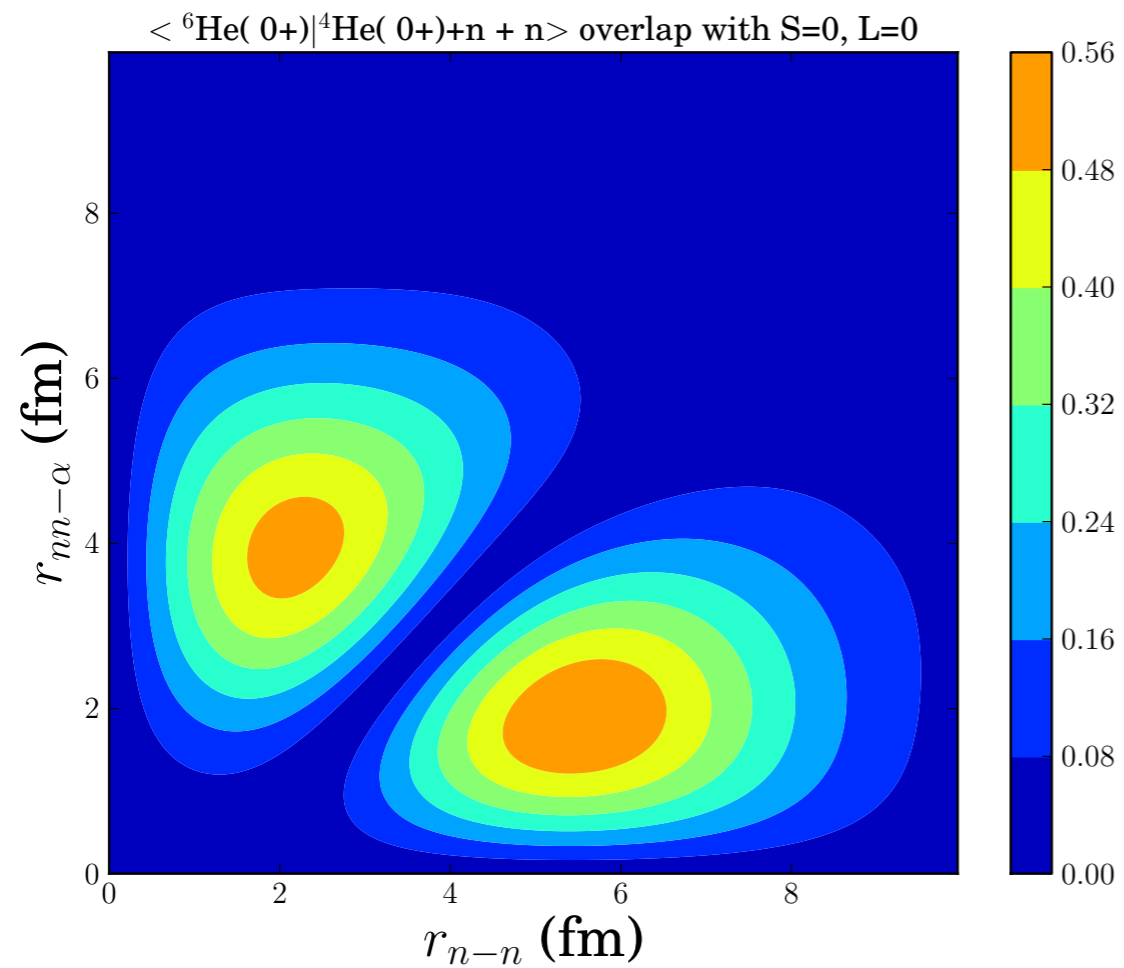
Ab initio $\langle {}^6\text{He} \mid {}^4\text{He}+n+n \rangle$ overlap

$N^3\text{LO}$, SRG

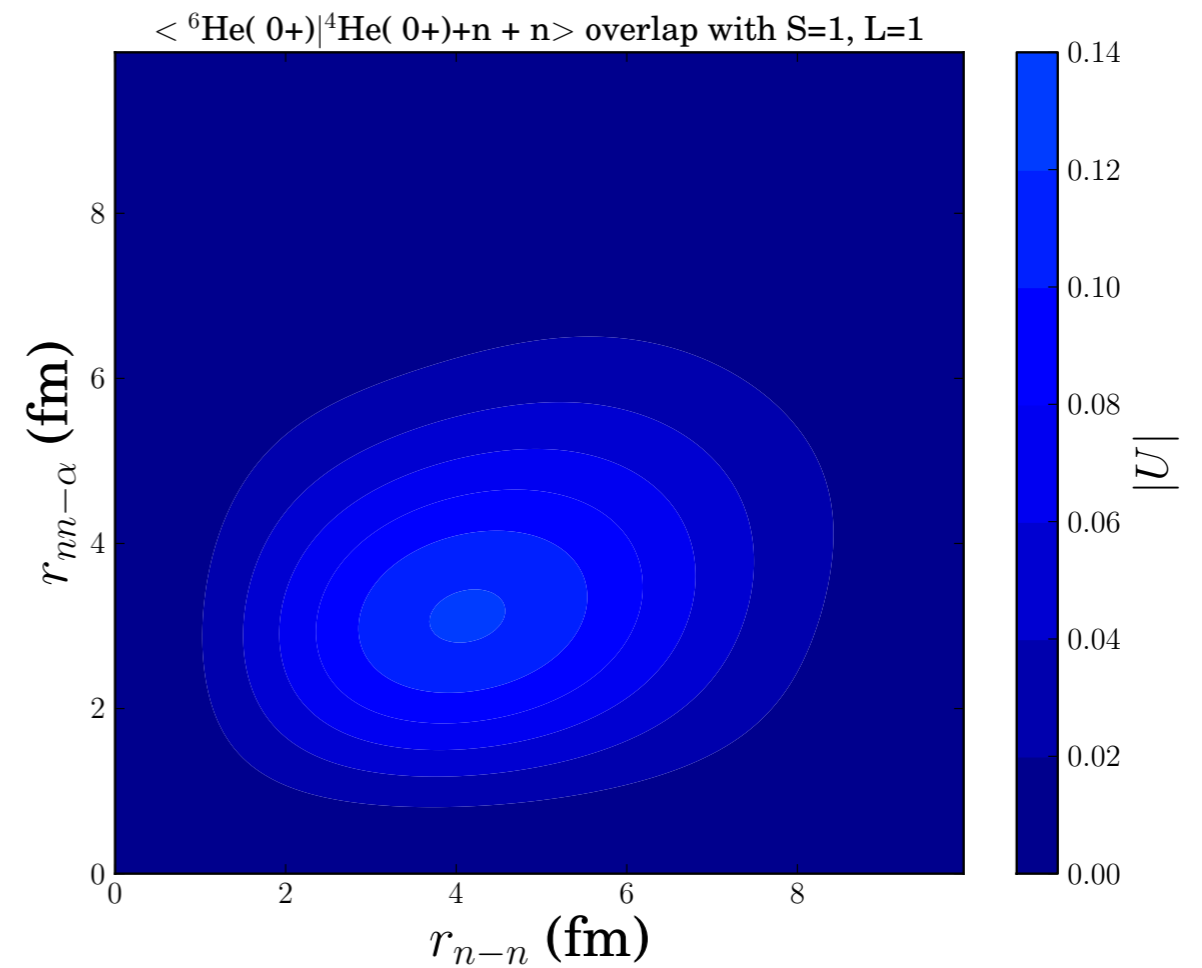
NN only, $\Lambda = 2.0 \text{ fm}^{-1}$,

$N_{\text{max}}=14$, HO=20 MeV

$\langle {}^6\text{He} (0^+) \mid {}^4\text{He} (0^+) + n + n \rangle$



$L=S=0$

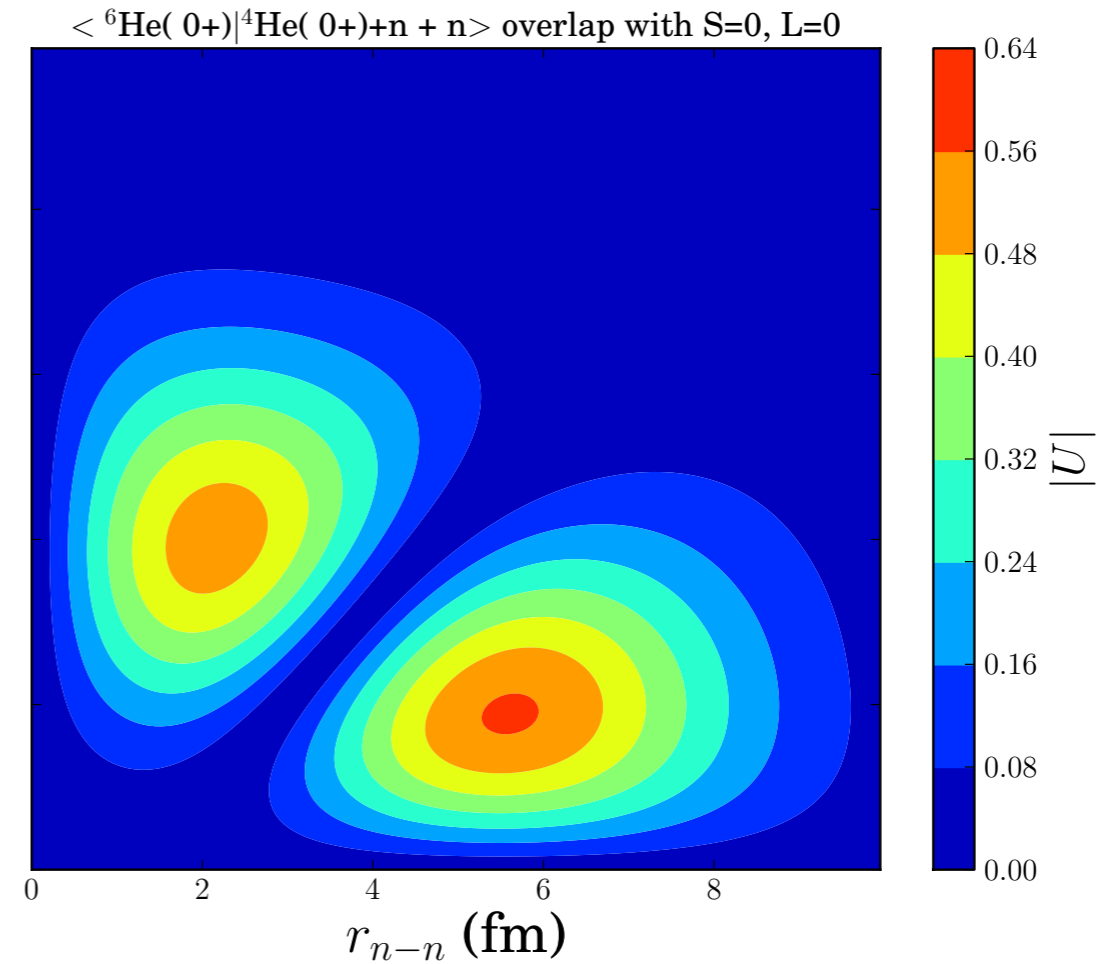
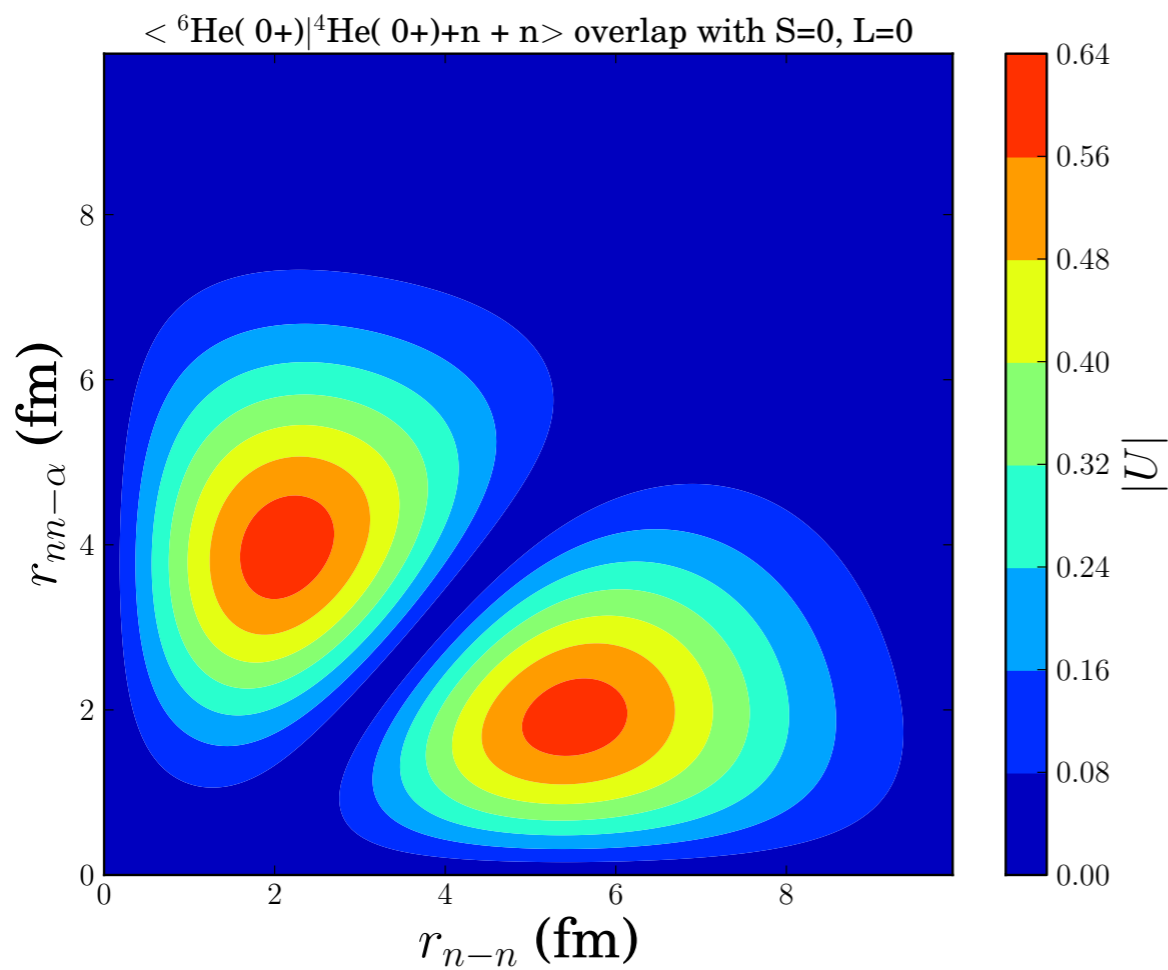


$L=S=1$

Ab initio $\langle {}^6\text{He} | {}^4\text{He}+n+n \rangle$ overlap

$N^3\text{LO}$, NN only
SRG, $\Lambda = 2.0 \text{ fm}^{-1}$,
 $N_{\text{max}}=8$, HO=16 MeV

$N^3\text{LO}$, NN+3NF
SRG, $\Lambda = 2.0 \text{ fm}^{-1}$,
 $N_{\text{max}}=8$, HO=16 MeV

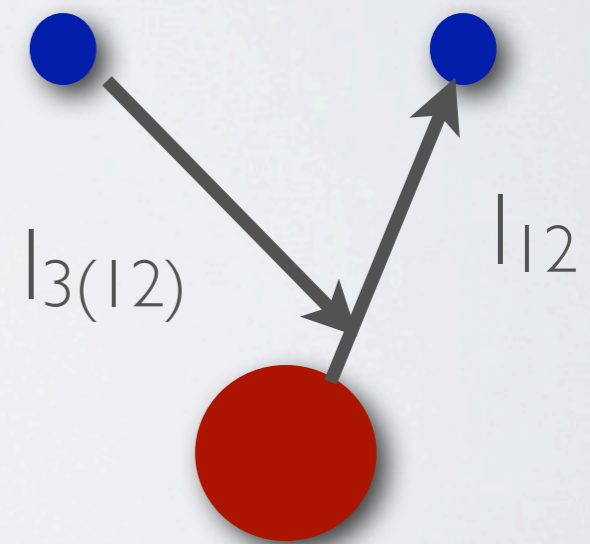
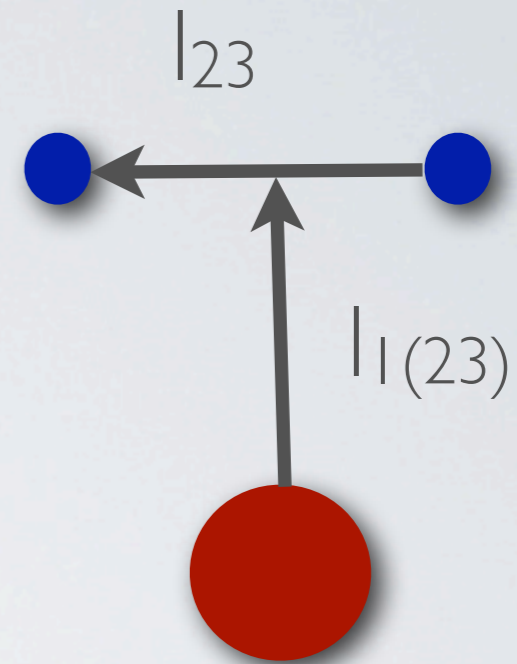


with 3NF

Pauli focusing

$$\langle {}^6\text{He} (0^+) | {}^4\text{He} (0^+) + n + n \rangle$$

- ❖ Dominance of the $l_{1(23)} = l_{23} = 0$ component.
- ❖ RR coefficients determine HH under coordinate-system transformation.
- ❖ E.g. with $l_{1(23)} = l_{23} = 0$ we get:
 - ▶ $l_{3(12)} = l_{12} = 0$ for $K=0$
(almost Pauli forbidden)
 - ▶ Dominating $l_{3(12)} = l_{12} = 1$ for $K=2$
 - ▶ Hyperangular function for this component gives the two-peak correlation density.



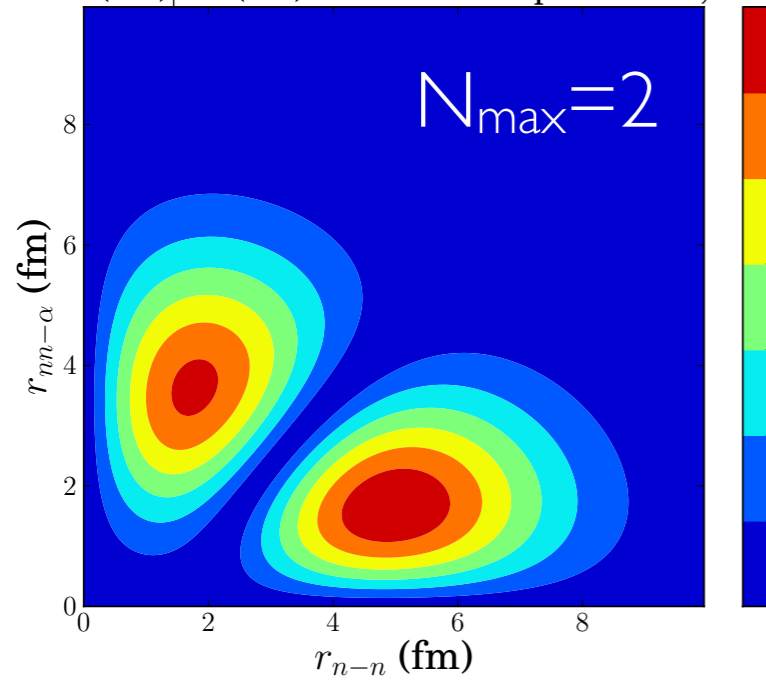
$\langle {}^6\text{He} | {}^4\text{He}+n+n \rangle$ overlap: N_{max} dependence

$$\langle {}^6\text{He} (0^+) | {}^4\text{He} (0^+) + n + n \rangle$$

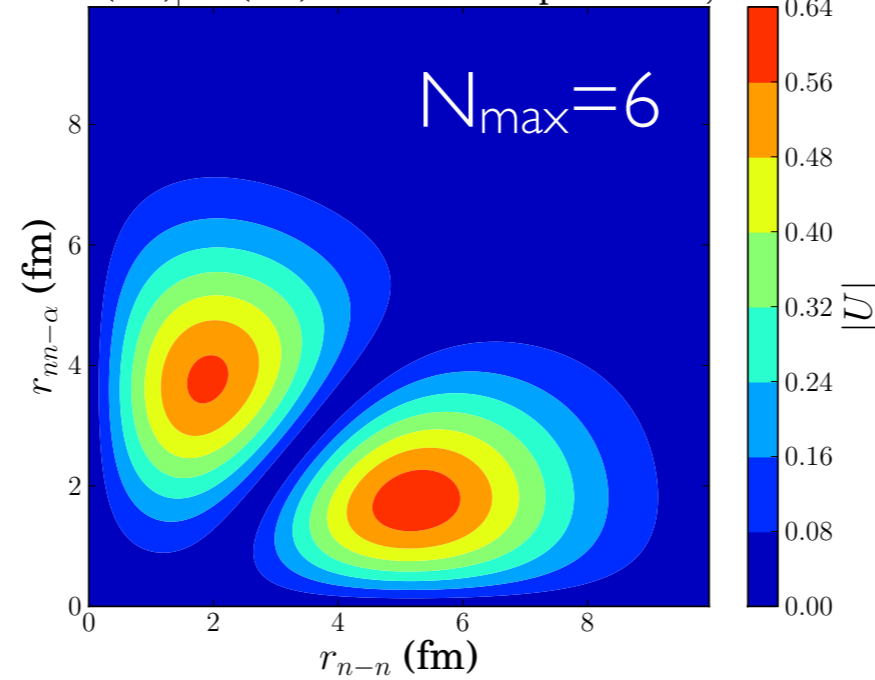
$N^3\text{LO}$, SRG

NN only, $\Lambda = 2.0 \text{ fm}^{-1}$,
 $N_{\text{max}} = 14$, HO = 20 MeV

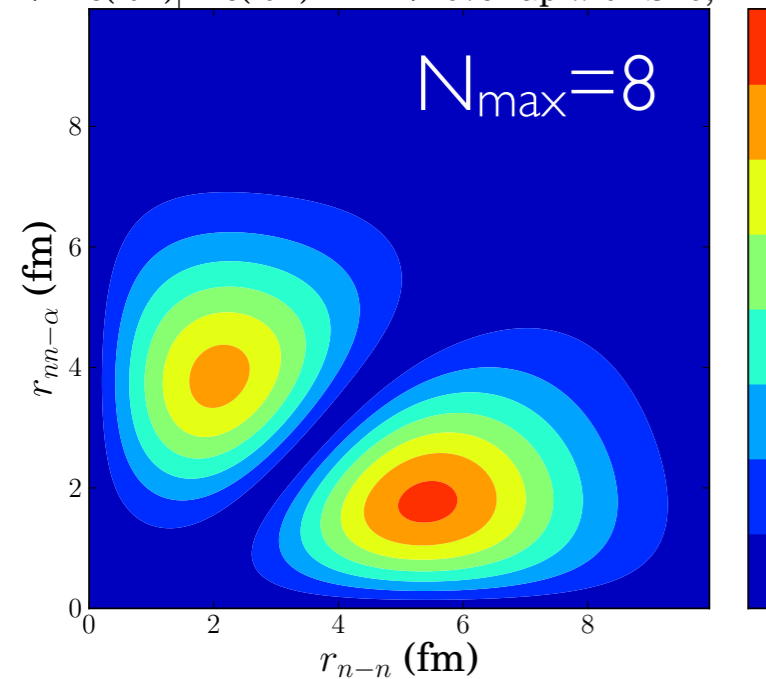
$\langle {}^6\text{He} (0^+) | {}^4\text{He} (0^+) + n + n \rangle$ overlap with $S=0, L=0$



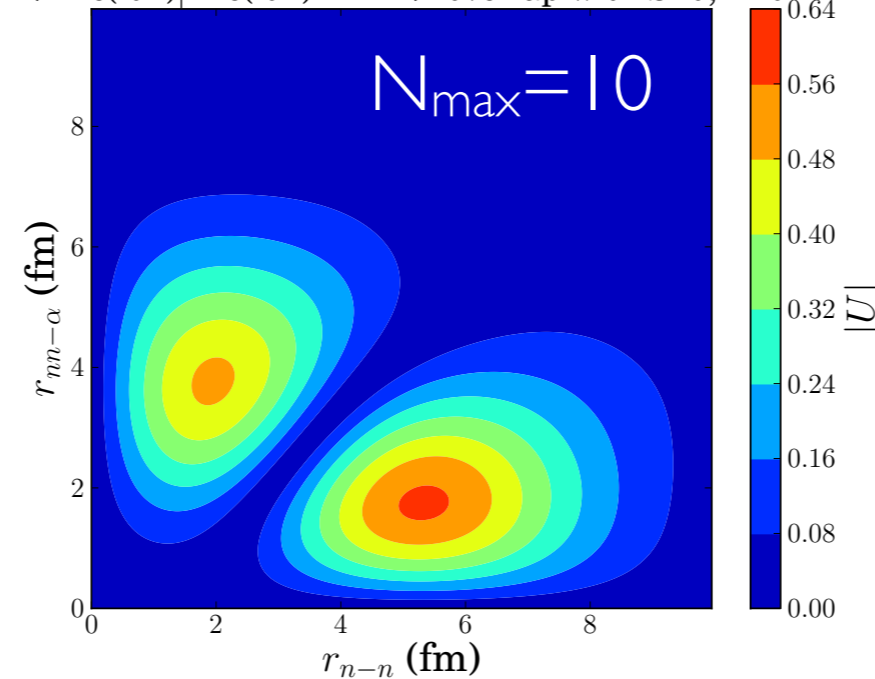
$\langle {}^6\text{He} (0^+) | {}^4\text{He} (0^+) + n + n \rangle$ overlap with $S=0, L=0$



$\langle {}^6\text{He} (0^+) | {}^4\text{He} (0^+) + n + n \rangle$ overlap with $S=0, L=0$



$\langle {}^6\text{He} (0^+) | {}^4\text{He} (0^+) + n + n \rangle$ overlap with $S=0, L=0$



Conclusion:
This is a Pauli
focusing effect

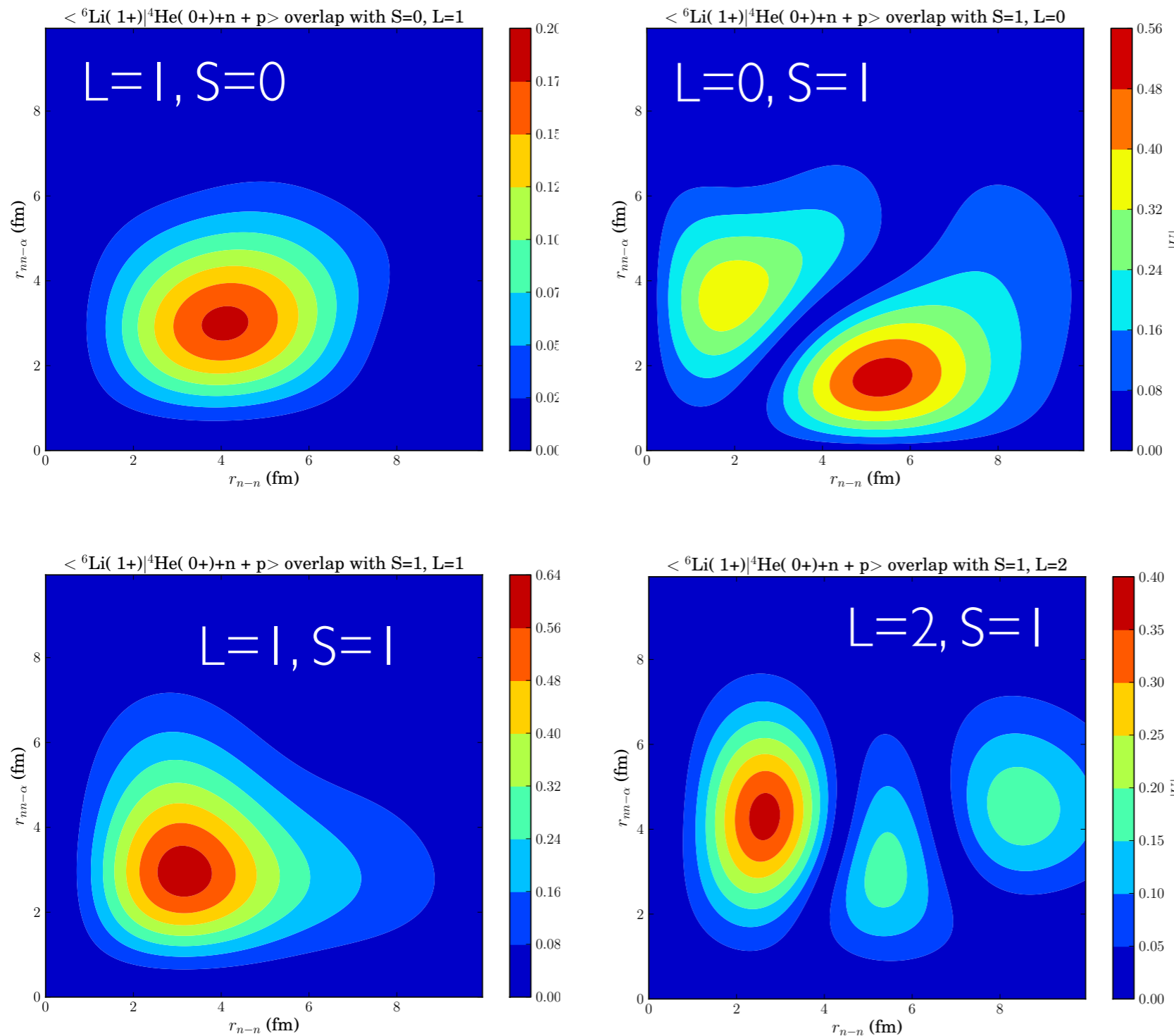
Ab initio $\langle {}^6\text{Li} \mid {}^4\text{He}+n+p \rangle$ overlap

$$\langle {}^6\text{Li} (1^+) \mid {}^4\text{He} (0^+) + n + n \rangle$$

$N^3\text{LO}$, SRG

NN only, $\Lambda = 2.0 \text{ fm}^{-1}$,

$N_{\text{max}} = 14$, HO = 20 MeV



Note: different scales

Conclusion and Outlook

- ❖ Introduction of UV and IR scales - Combination of results from different N_{\max} , $\hbar\Omega$
- ❖ Optimization of run sequence - BUT still need several large N_{\max} computations
- ❖ Prefer UV converged results and perform IR extrapolation
- ❖ Study of tw-body operators, and the transformation of operators
- ❖ Microscopic description of clustering
 - ▶ Calculate core swelling: r_{pp}
 - ▶ Study projection on HH basis
- ❖ Continuum effects in ab initio calculations

Acknowledgments

Many thanks to my collaborators

- ❖ Lucas Platter (ANL), Jimmy Rotureau, Mikhail Zhukov, Emil Ryberg, **Daniel Sääf**, Boris Carlsson (Chalmers) <http://fy.chalmers.se/subatom/nt>
- ❖ Petr Navrátil (TRIUMF), Robert Roth (Darmstadt), James Vary and Pieter Maris (Iowa), and the NCSM collaboration.
- ❖ Witek Nazarewicz and Nicolas Michel (UT/ORNL), Marek Ploszajczak (GANIL), George Papadimitriou and Bruce Barrett (UA)

CHALMERS



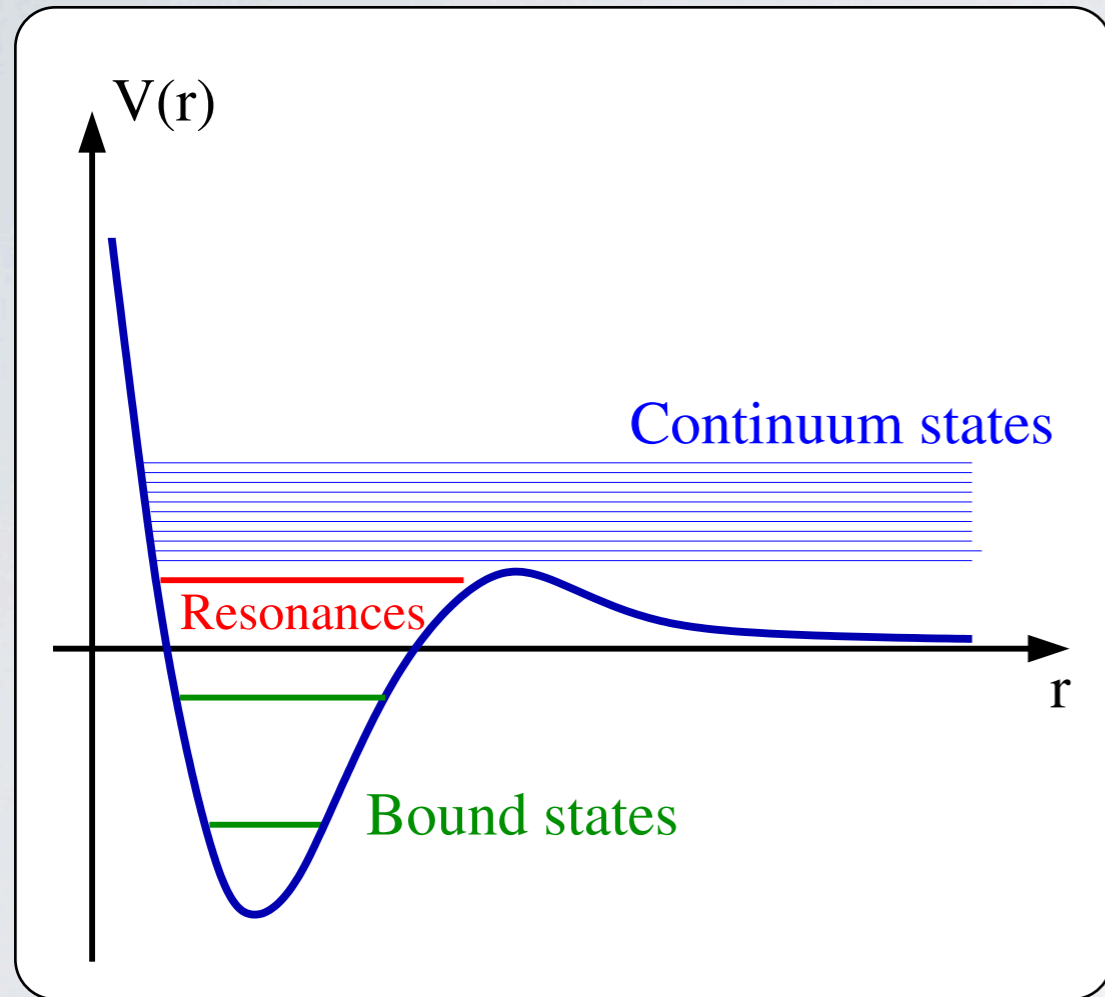
Research funded by:

- The Swedish Research Council
- European Research Council

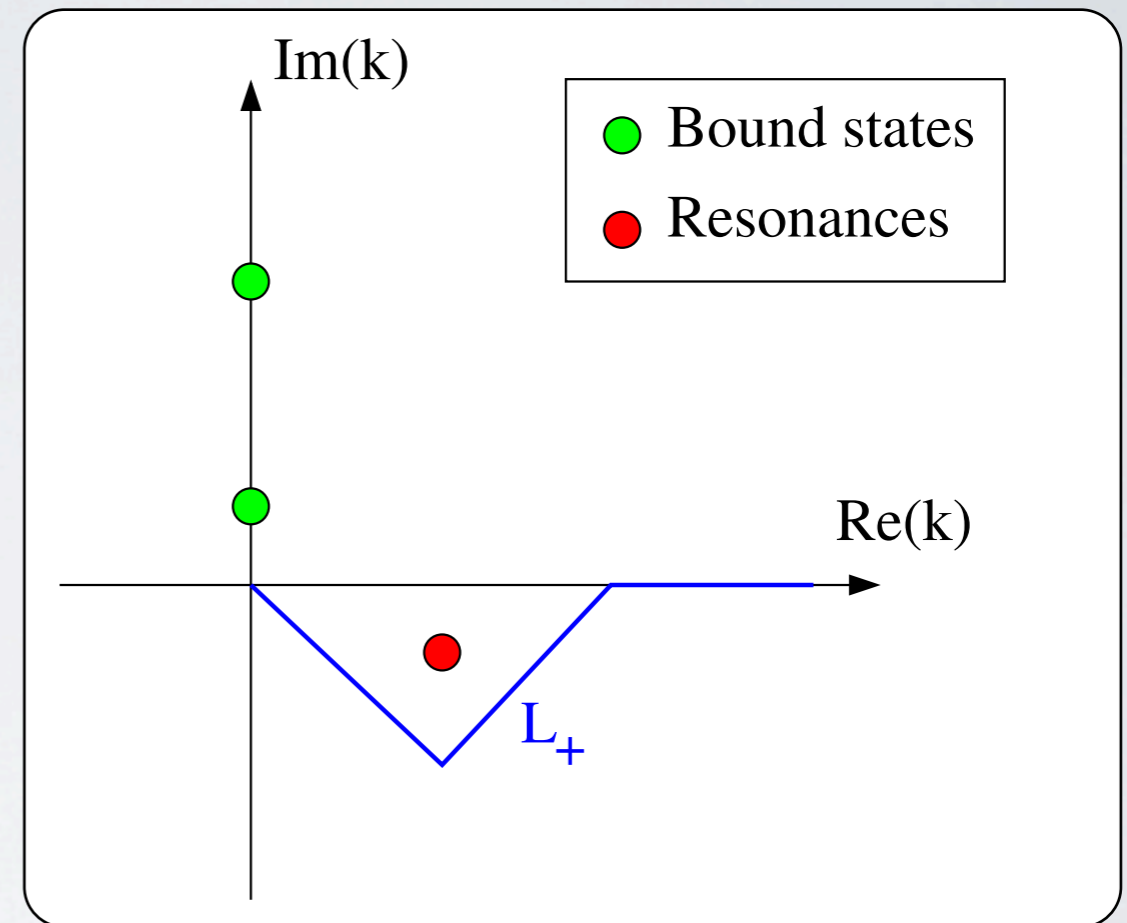
Stepping Into The Continuum

Gamow states and the Berggren basis

Gamow Shell Model



Berggren basis



Gamow Shell Model

- N. Michel et al Phys. Rev. Lett. **89**(2002) 042502;
- J. Rotureau et al. (2006)
- G. Hagen et al. (2010)

$$\sum_{n=b,r} |u_n\rangle\langle\bar{u}_n| + \frac{1}{\pi} \int_{L_+} |u(k)\rangle\langle u^*(k)| dk = 1$$

Gamow states and completeness

- T. Berggren, Nucl. Phys A **109**(1968)265; NPA**389**(1982)261
- T. Lind, Phys. Rev. C **47**(1993)1903

Gamow shell Model

- (i) discretization of continuum contour

$$\sum_{n=b,r} |u_n\rangle\langle u_n| + \sum_i |u_{k,i}\rangle\langle u_{k,i}| \approx 1$$

- (ii) construction of many-body basis

$$|\mathbf{SD}_i\rangle = |u_{i1}, \dots, u_{iA}\rangle$$

- (iii) construction of Hamiltonian matrix (complex symmetric matrix)

$$\langle \mathbf{SD}_i | H | \mathbf{SD}_j \rangle$$

- (iv) many-body spectrum contains: bound, resonant and “spurious” continuum states

Gamow Shell Model

- N. Michel et al, PRL 89 (2002) 042502; PRC67 (2003) 054311; PRC70 (2004) 064313; JPG (2009) 013101
- G. Hagen et al, PRC71 (2005) 044314
- J. Rotureau et al, PRL 97 (2006) 110603
- G. Papadimitriou et al, PRC(R) 84 (2011) 051304

- Pole approximation is 0th order approximation:

$$H^{\text{p.a.}} |\Psi^{\text{p.a.}}\rangle = E^{\text{p.a.}} |\Psi^{\text{p.a.}}\rangle$$

- Many-body resonance (bound) state have large overlap:

$$|\langle \Psi^{\text{p.a.}} | \Psi \rangle|$$

ab initio Calculations in the Berggren Basis

❖ NN potential

- ▶ Realistic 2b interactions V_{ij} : Argonne V18 or chiral I-N³LO
- ▶ softened by $V_{\text{low-k}}$

❖ Single-particle states

- ▶ s- and p-shells from HF potential
- ▶ $l > 1$ shells from HO potential

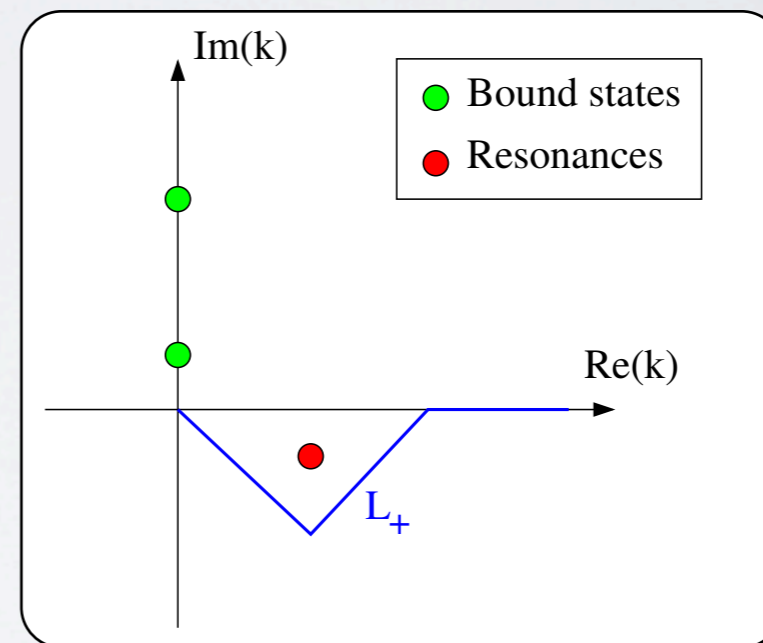
❖ Diagonalization

- ▶ many-body Schrödinger equation

$$H_A = \frac{1}{A} \sum_{i < j}^A \frac{(\vec{p}_i - \vec{p}_j)^2}{2m} + \sum_{i < j}^A V_{NN}(\vec{r}_i - \vec{r}_j) + \dots$$

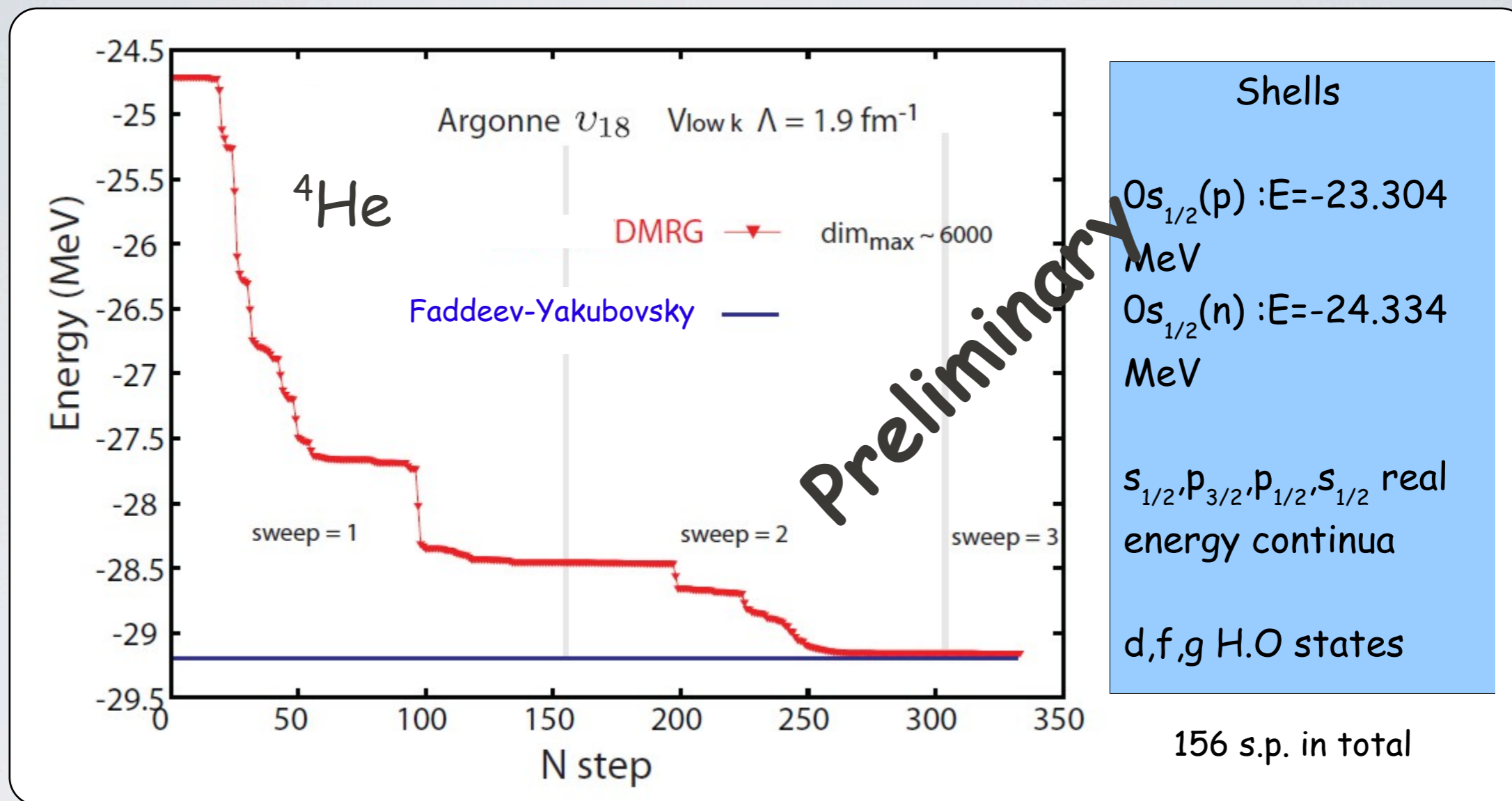
- ▶ using J-coupled DMRG (basis truncation)

- R. Wiringa et al., Phys. Rev. C, **51**(1995)38
- D. Entem et al., Phys. Rev. C, **68**(2003)041001(R)
- S. Bogner et al., Phys. Rep., **386**(2003)1
- J. Rotureau et al., Phys. Rev. Lett., **97**(2006)110603

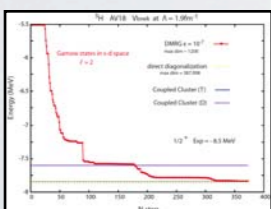


Ab initio Benchmark calculations in a Gamow Basis

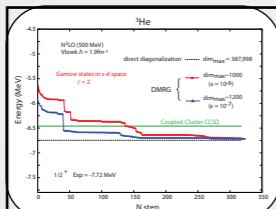
^4He



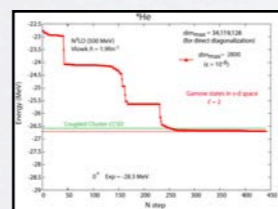
^3H



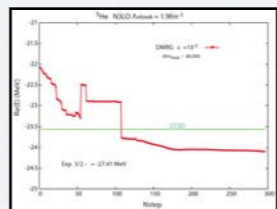
^3He



^4He



^5He

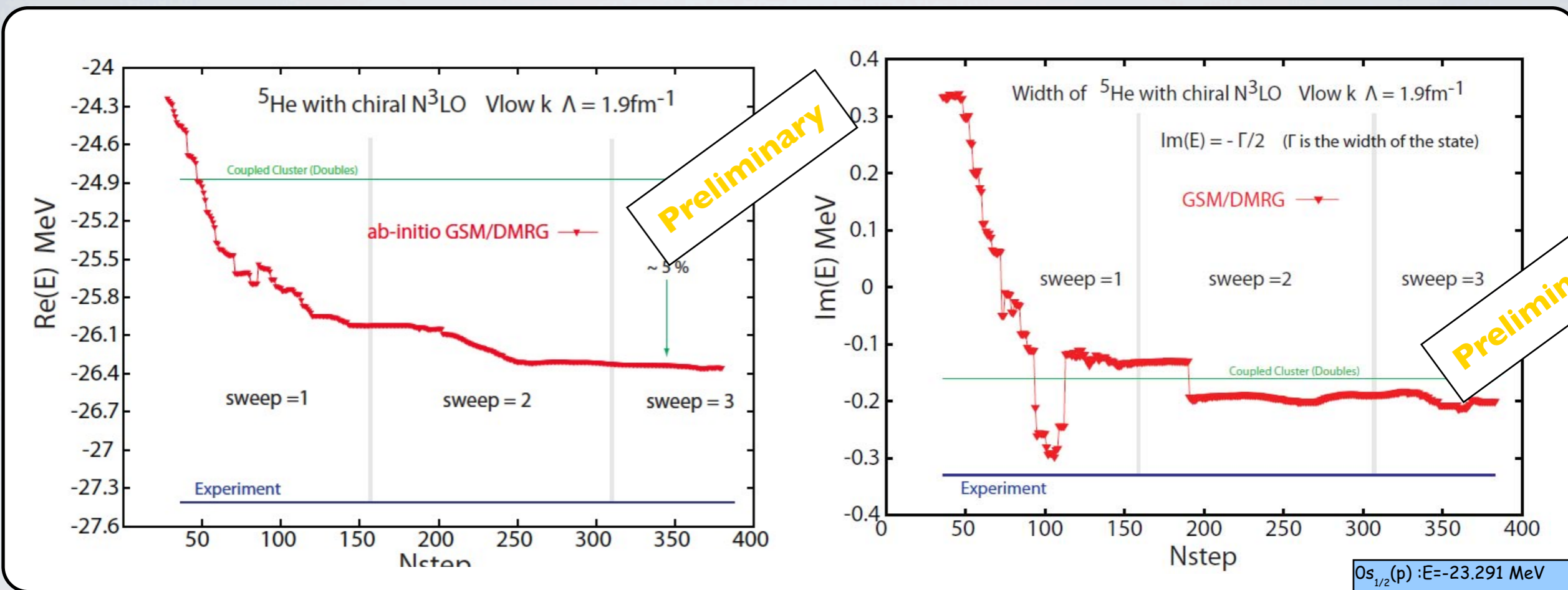


Ab initio NCGSM:

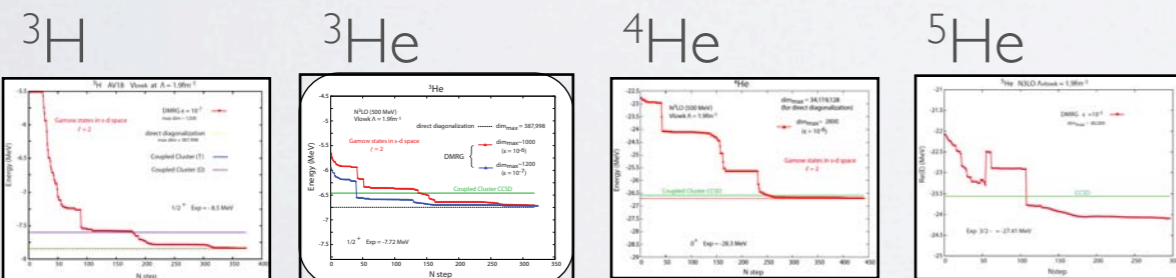
- **G. Papadimitriou, J. Rotureau**, B. Barrett, M. Ploszajczak, W. Nazarewicz, N. Michel
- See FUSTIPEN workshop, March 2012

Ab initio Benchmark calculations in a Gamow Basis

^5He



$0s_{1/2}(p)$: $E = -23.291$ MeV
 $0s_{1/2}(n)$: $E = -23.999$ MeV
 $0p_{3/2}(n)$: $E(1.194, -0.633)$
 $p_{3/2}(n)$ complex contour (discretized)
 $s_{1/2}, p_{3/2}, p_{1/2}, s_{1/2}$ real energy continua
 d, f, g H.O states
 157 s.p. in total



Ab initio NCGSM:

- **G. Papadimitriou, J. Rotureau**, B. Barrett, M. Płoszajczak, W. Nazarewicz, N. Michel
- See FUSTIPEN workshop, March 2012